Electronic Supplementary Material (ESI) for Journal of Materials Chemistry C.
This journal is © The Royal Society of Chemistry 2022

# Electronic Supplementary Information

# Discovery of Resonance-Enhanced Emission Effect and its Application in Fluorescent Molecule Design

**Xue Liu[a], Wei Ye[a], Wan Lin[b,c,d], Yinwei Cheng[b,c,d], Liyan Xu[b,c,d], Enmin Li[c], Hefeng Zhang*[a,e]**

[a]Department of Chemistry, Key Laboratory for Preparation and Application of Ordered Structural Materials of Guangdong Province, College of Science, Shantou University, Shantou, 515063, China;

[b]Guangdong Esophageal Cancer Research Institute, Shantou Sub-center, Cancer Research Center, Shantou University Medical College, Shantou, 515041, China;

[c]Guangdong Provincial Key Laboratory of Infectious Diseases and Molecular Immunopathology, Institute of Oncologic Pathology, Shantou University Medical College, Shantou, 515041, China;

[d]The Key Laboratory of Molecular Biology for High Cancer Incidence Coastal Chaoshan Area, Department of Biochemistry and Molecular Biology, Shantou University Medical College, Shantou, 515041, China;

[e]Guangdong Provincial Laboratory of Chemistry and Fine Chemical Engineering, Shantou, 515063, China. * Corresponding author, email: hfzhang@stu.edu.cn

## Table of Contents

## 1. Experimental methods

*Materials and Instruments*

All chemical and reagents were purchased from Aladdin Chemical Company. UV-Vis spectra were recorded on a Shimadzu UV-2600 UV-Visible spectrophotometer. Fluorescence spectra (<900nm) were measured on an F-7000 FL spectrophotometer. Proton and carbon nuclear magnetic resonance spectra ($^{1}$H-NMR and $^{13}$C-NMR) were recorded on an AVANCE-400 MHz and 100 MHz NMR spectrometer, respectively, with TMS as an internal reference. Compounds were routinely checked by thin layer chromatography (TLC) on silica gel plates using chloroform: methanol. The crude products were purified by flash column chromatography and re-crystallization techniques.

*Sample preparation*

Unless otherwise specified, the sample solution prepared by transferring a probe solution of 20 μL of DMSO and configure it to a concentration of 10 mmol/mL in different solvent.

*Synthetic scheme*

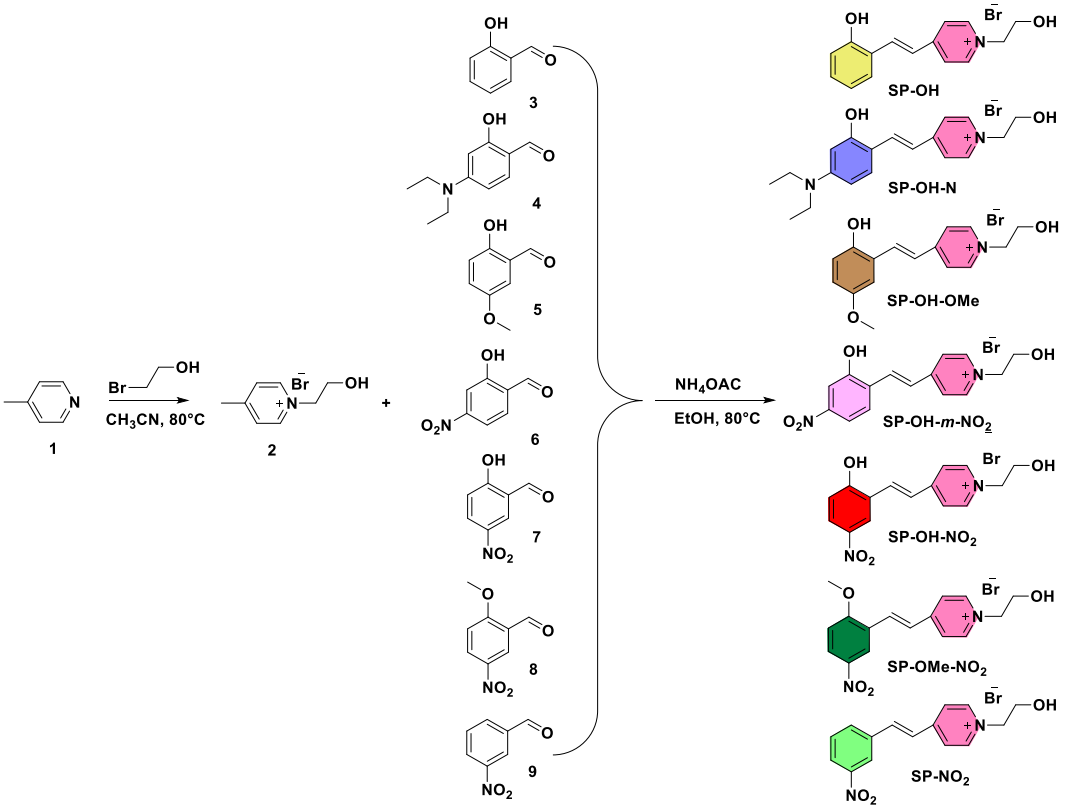


**Scheme S1.** Synthesis of SP-OH and its derivatives of SP-OH-N,SP-OH-OMe, SP-OH-*m*-$NO_2$, SP-OH-$NO_2$, SP-OMe-$NO_2$ and SP- $NO_2$ by coupling aldehyde in salicylaldehyde and methyl group in pyridinium substrate.

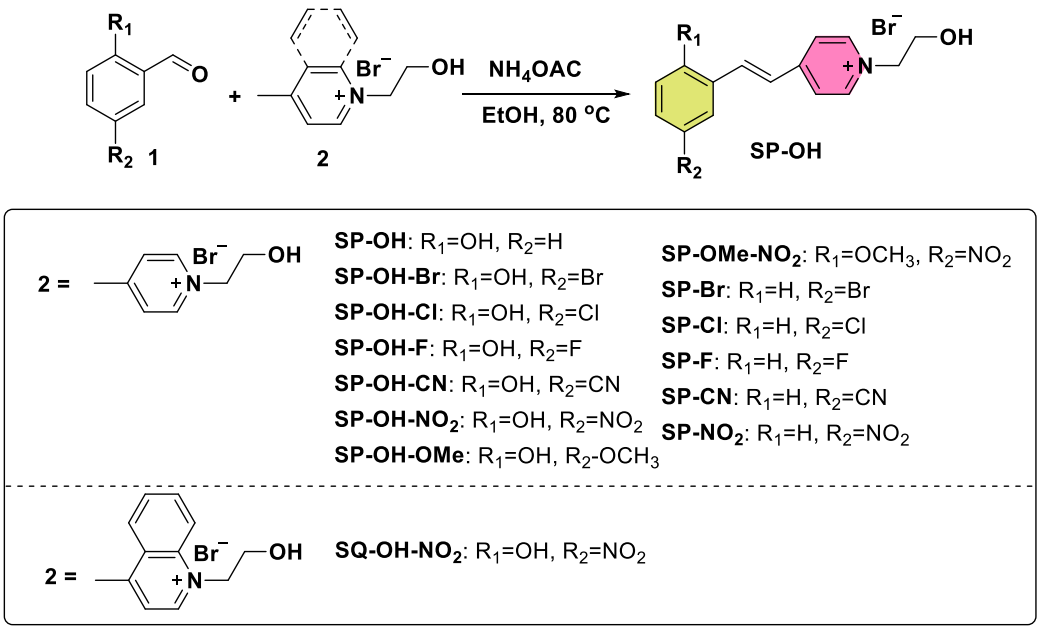


**Scheme S2.** General synthesis route of SP-OH derivatives fluorescence probe.

## 2. Supplementary tables and figures

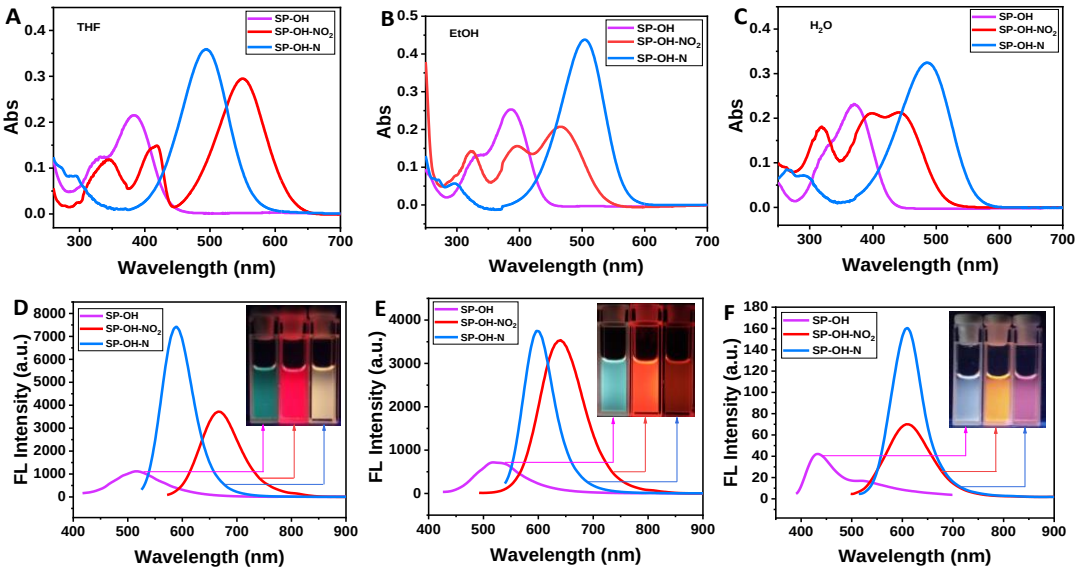


**Figure S1.** The UV absorption spectra (A-C) and fluorescence spectra (D-F) ($c$ = 10 mmol/mL) of compounds SP-OH, SP-$NO_2$-OH and SP-OH-N in different solvents (THF, EtOH, $H_2O$). Inset: Picture of compound in 365 nm UV light.

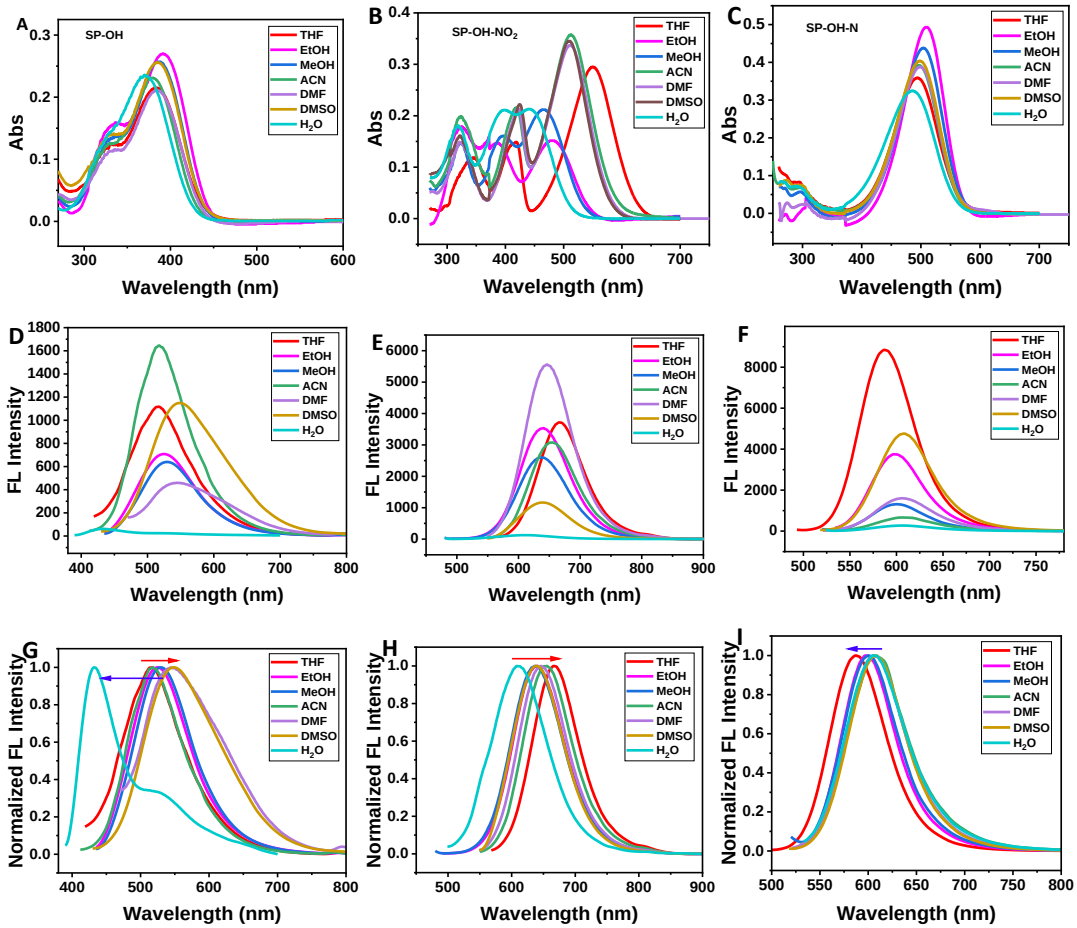


**Figure S2.** The UV absorption spectra (A-C) and fluorescence emission spectra (D-F) and fluorescence normalized spectra (G-H) of compounds SP-OH, SP-OH-$NO_2$ and SP-OH-N in different solvents ($c$ = 10 mmol/mL) (tetrahydrofuran (THF), anhydrous ethanol (EtOH), anhydrous methanol (MeOH), acetonitrile (ACN), dimethylformamide (DMF), dimethyl sulfoxide (DMSO), water ($H_2O$).

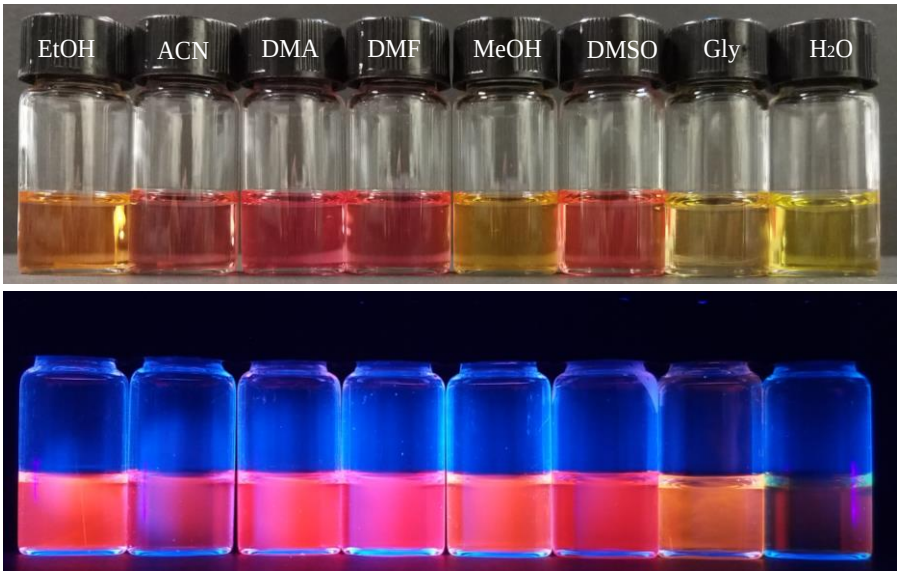


**Figure S3.** Fluorescence photograph of SP-OH-$NO_2$ in different solvents under daylight (top) or 365 nm UV lamp (bottom).

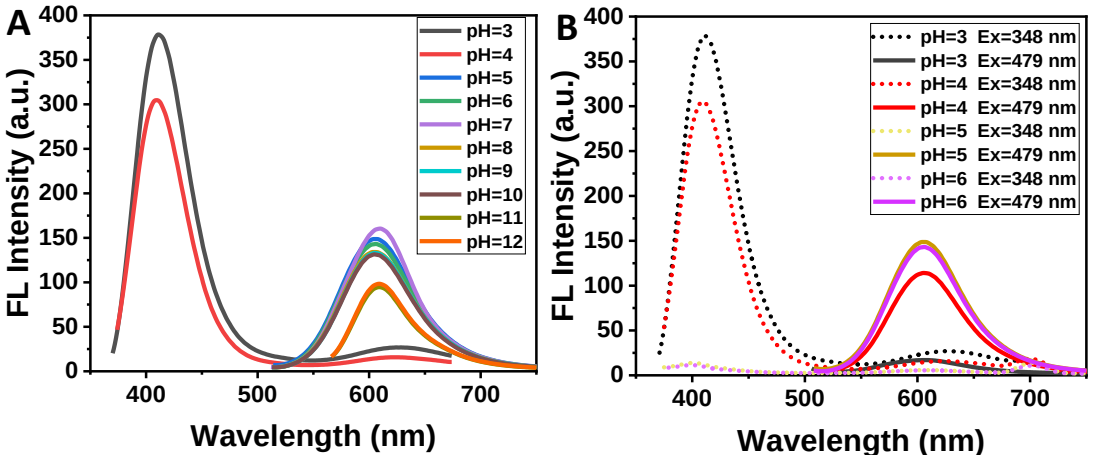


**Figure S4.** Fluorescence emission spectra of compound SP-OH-N ($c$ = 10 mmol/mL) under different excitation conditions. A) pH = 3-4, $\lambda_{ex}$ = 348 nm; pH = 5-12, $\lambda_{ex}$ = 479 nm; B) pH = 3-6 (Dashed line: $\lambda_{ex}$ = 348 nm , solid line: $\lambda_{ex}$ = 479 nm).

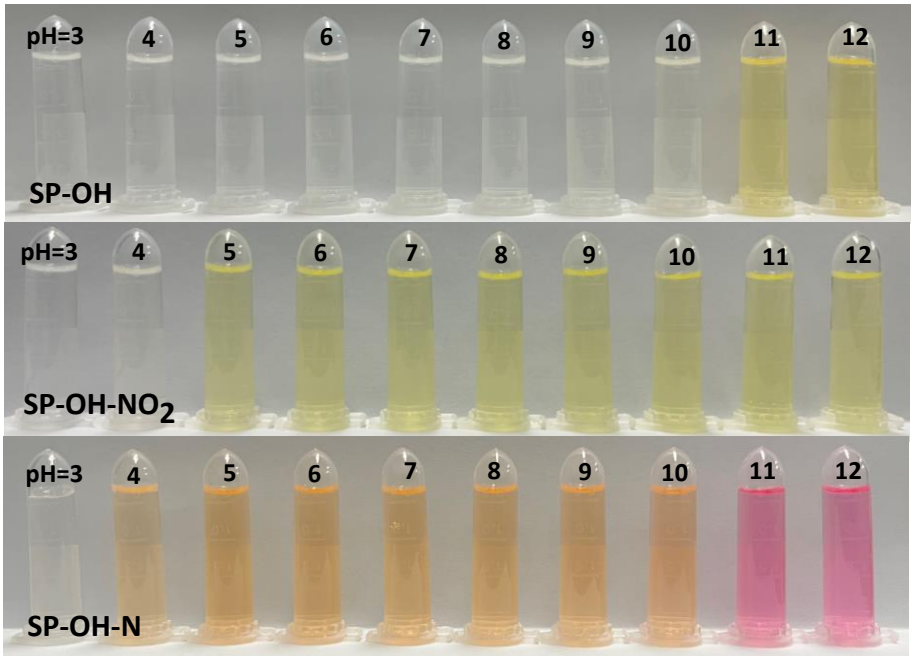


**Figure S5.** Photographs of compounds SP-OH, SP-OH-$NO_2$ and SP-OH-N at different pH values ($c$ = 10 mmol/mL).

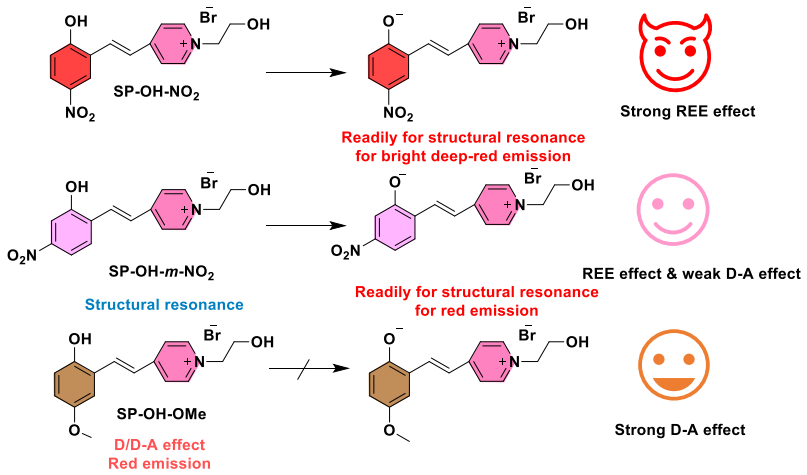


**Figure S6.** Possible mechanism of difference in luminescence behavior between SP-OH-$NO_2$, SP-OH-$m$-$NO_2$ and SP-OH-OMe.

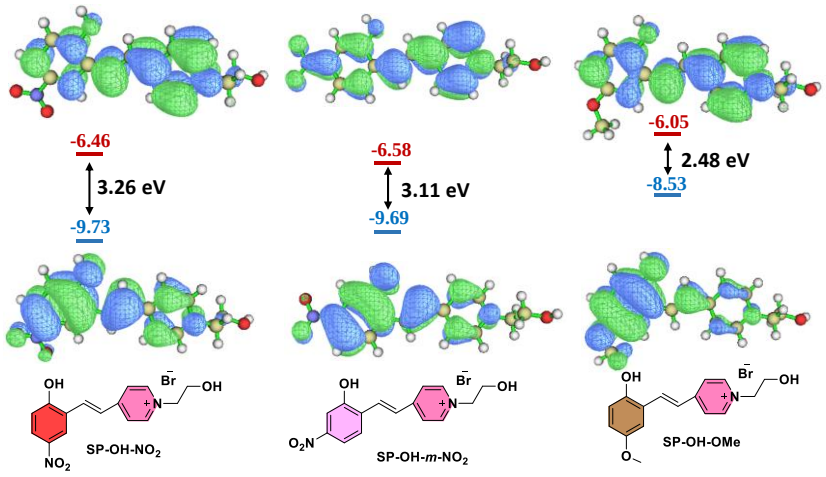


**Figure S7.** Chemical structures and HOMO-LUMO energy level diagrams of SP-OH-$NO_2$, SP-OH-*m*-$NO_2$ and SP-OH-OMe.

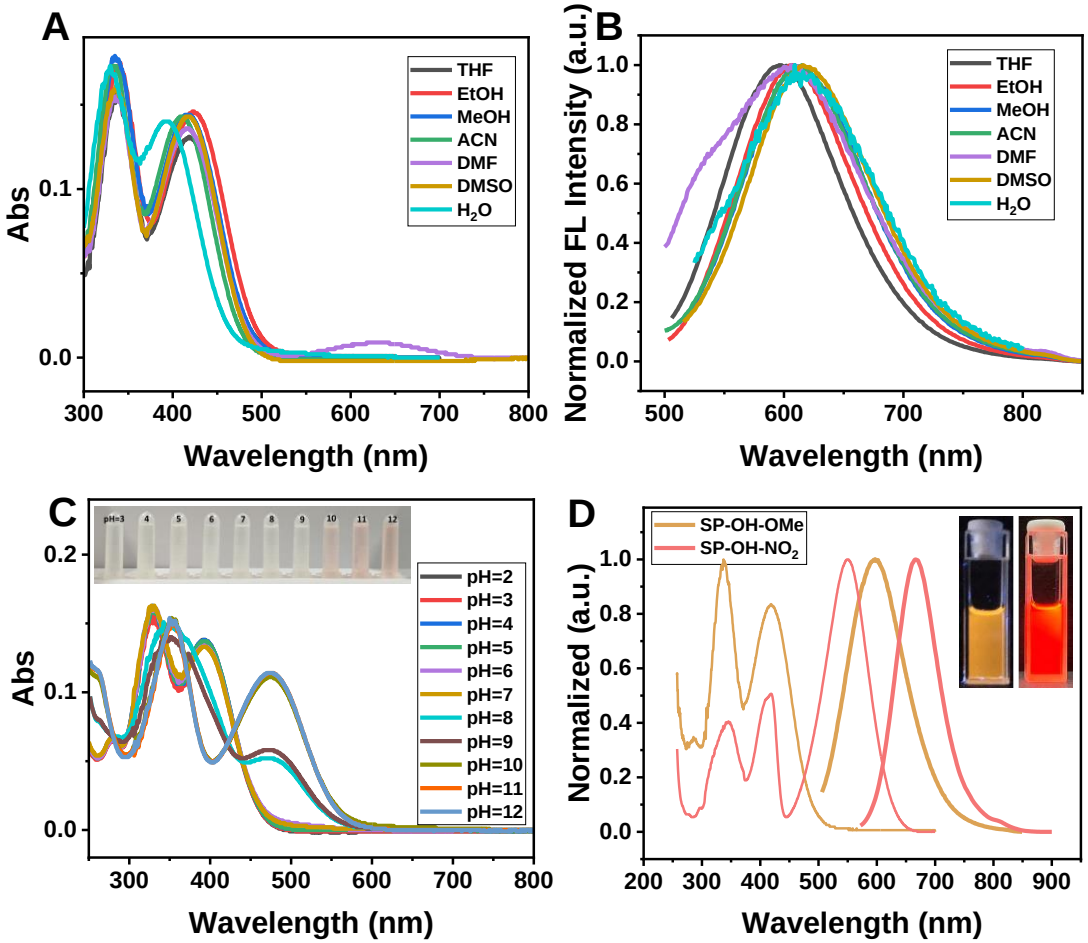


**Figure S8.** The UV-Vis absorption (A) and fluorescence spectra (B) of SP-OH-OMe ($c$ = 10 mmol/mL) in different solvents; (C) The UV-Vis absorption at different pH environment (Its fluorescence in water is too weak to be detected); (D) Absorption (left lines) and fluorescence emission spectra (right lines) of SP-OH-OMe (yellow) and SP-OH-$NO_2$ (red) in tetrahydrofuran.

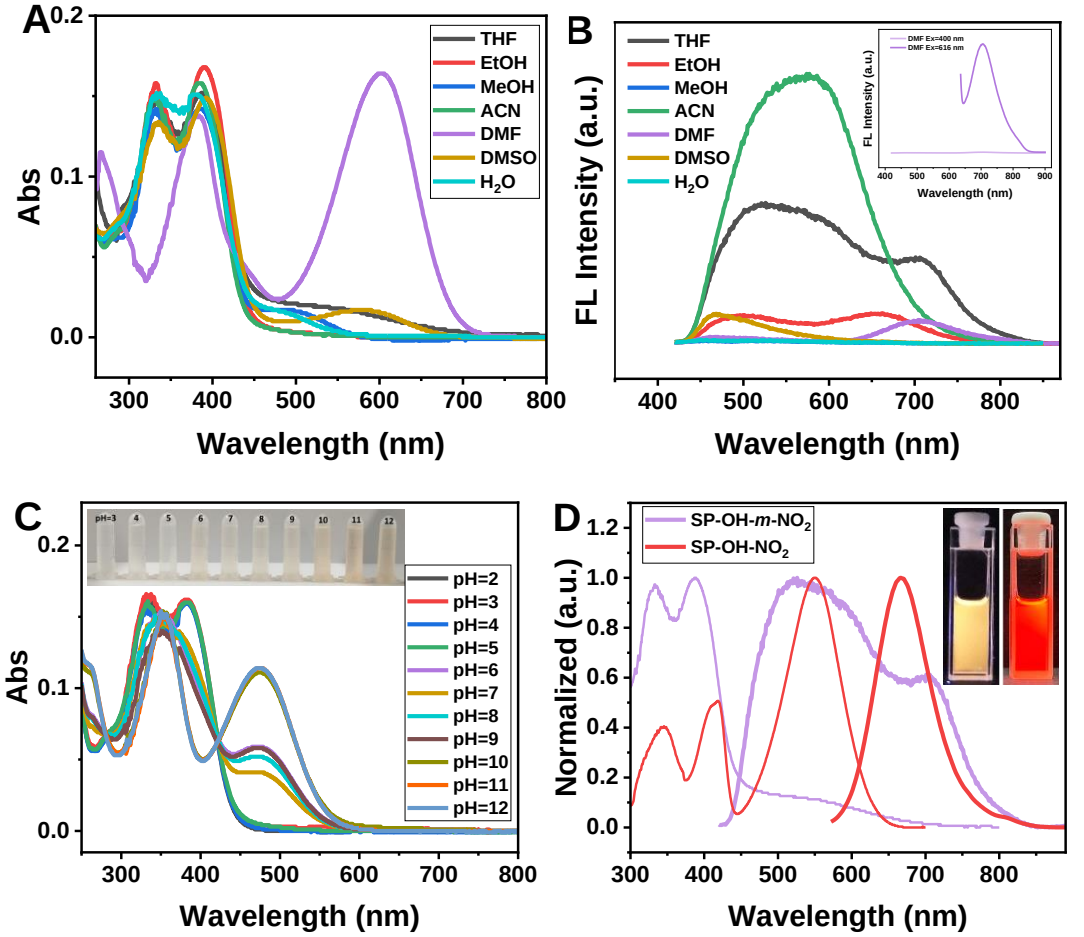


**Figure S9.** The UV-Vis absorption A) and fluorescence spectra B) of SP-OH-*m*-$NO_2$ ($c$ = 10 mmol/mL) in different solvents; C) The UV-Vis absorption at different pH environment (Its fluorescence in water is too weak to be detected); D) Absorption (left lines) and fluorescence emission spectra (right lines) of SP-OH-*m*-$NO_2$ (purple) and SP-OH-$NO_2$ (red) in tetrahydrofuran.

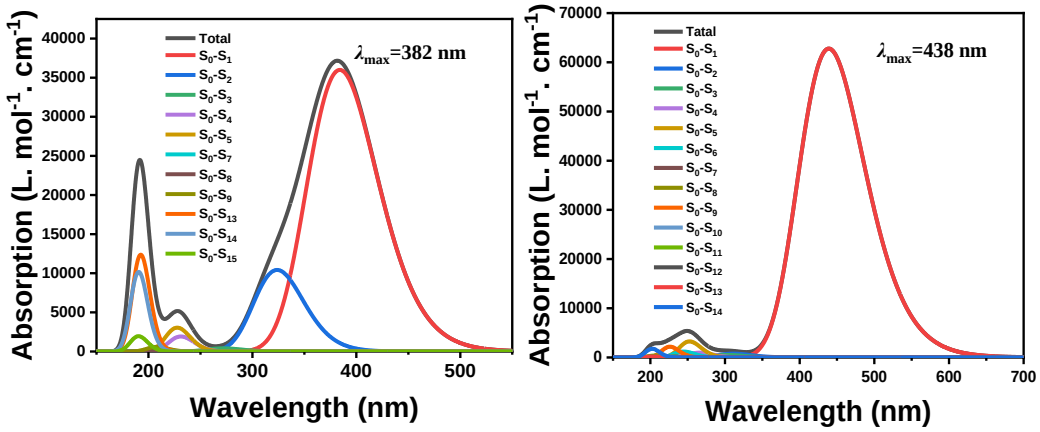


**Figure S10.** Contributions and total absorption spectra of ground state transitions of SP-OH (left) and SP-OH-N (right) to different excited states.

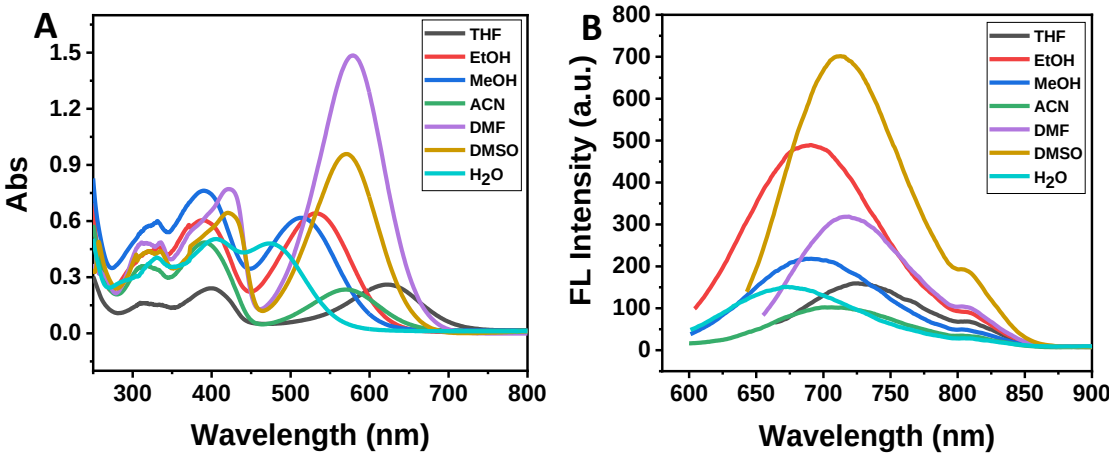


**Figure S11.** A) The UV-Vis absorption and B) fluorescence emission spectra of SQ-OH-$NO_2$ ($c$ = 50 mmol/mL) in different solvents.

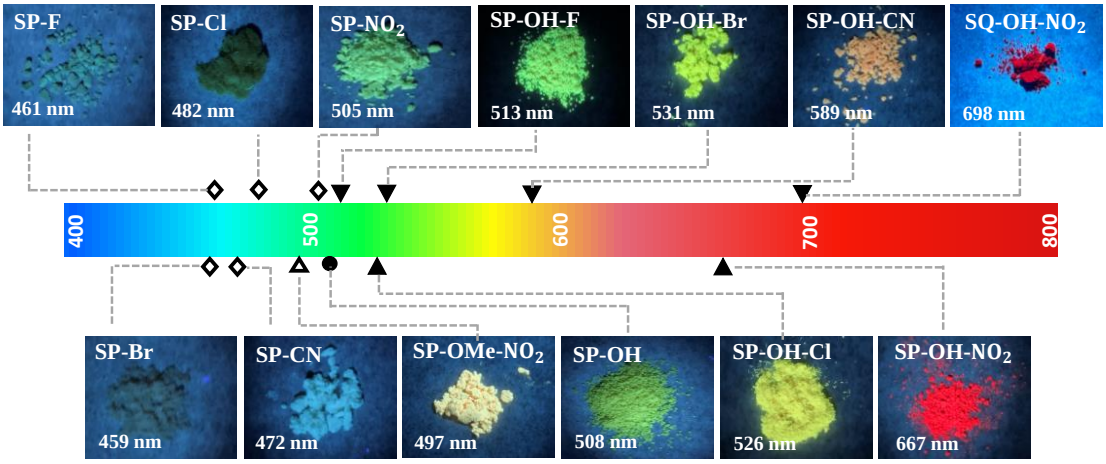


**Figure S12.** Fluorescence photograph of SP-OH derivative in solid under 365 nm UV lamp.

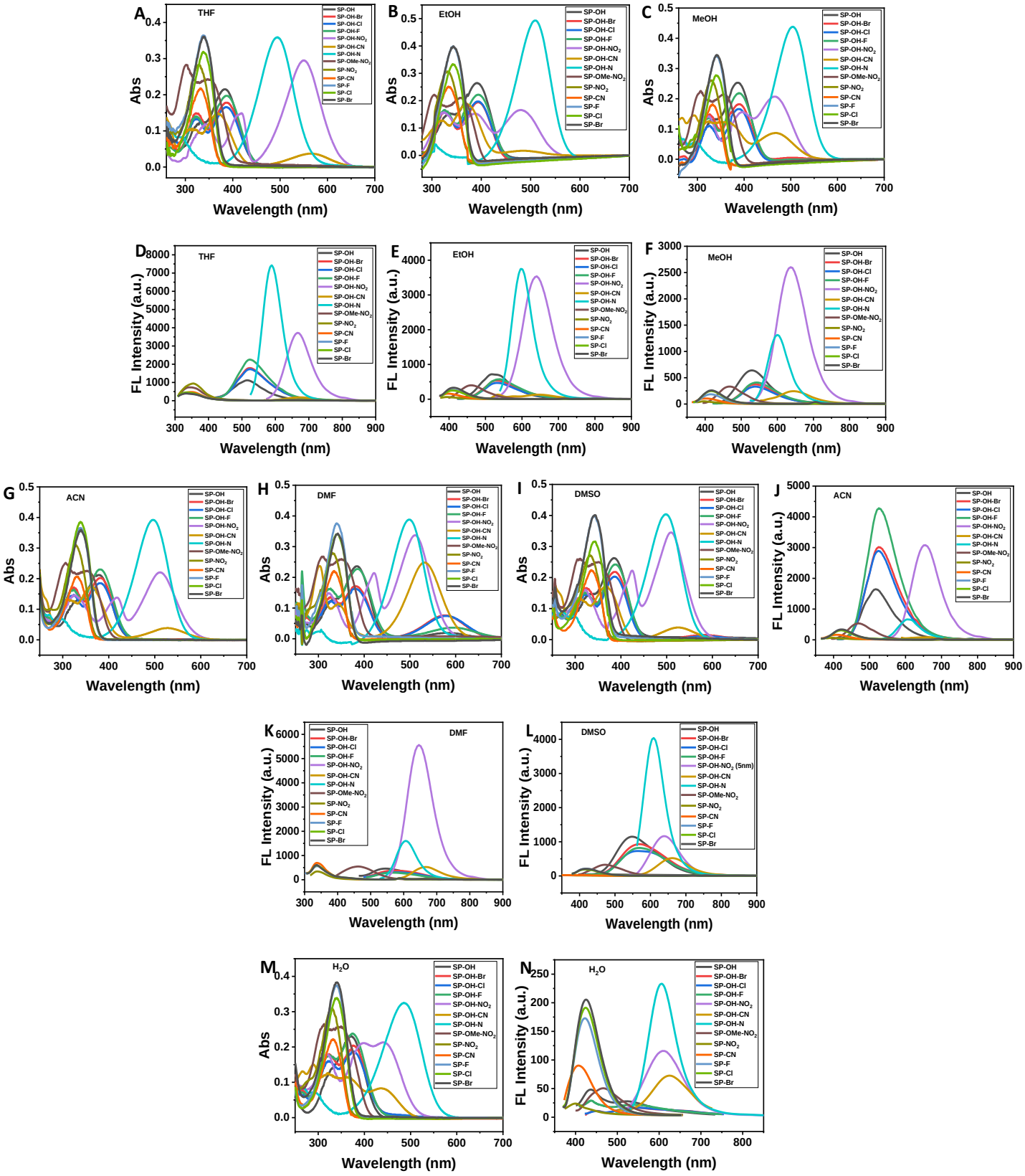


**Figure S13.** The UV-Vis absorption (A, B, C, G, H, I, M) and fluorescence spectra (B, E, F, J, K, L, N) of SP-OH derivatives ($c$ = 10 mmol/mL) in different solvents.

**Table S1.** The absorption wavelengths of SP-OH derivatives in different solvents

| Dyes | THF | EtOH | MeOH | ACN | DMF | DMSO | $H_2O$ |
|---|---|---|---|---|---|---|---|
| SP-OH | 383/329 | 391/334 | 386/331 | 378/331 | 384/332 | 385/329 | 370/326 |
| SP-OH-Br | 387/323 | 394/326 | 390/326 | 382/322 | 577/381/325 | 386/325 | 375/322 |
| SP-OH-Cl | 386/323 | 394/325 | 389/325 | 380/322 | 579/381/326 | 386/323 | 375/322 |
| SP-OH-F | 387/322 | 394/325 | 389/324 | 380/320 | 595/384/323 | 386/322 | 374/322 |
| SP-OH-CN | 564/369/313 | 484/370/320 | 469/366/294 | 526/362/308 | 532/384/323 | 525/367/309 | 439/364/322 |
| SP-OH-$NO_2$ | 549/416/344 | 480/388/324 | 465/395/323 | 512/417/324 | 511/420/322 | 509/424/321 | 442/396/318 |
| SQ-OH-$NO_2$ | 623/400/313 | 532/388/321 | 513/390/327 | 570/391/315 | 578/421/316 | 570/421/321 | 474/402/328 |
| SP-OH-N | 494 | 508 | 504 | 498 | 498 | 498 | 485 |
| SP-OMe-$NO_2$ | 352/301 | 358/304 | 358/306 | 353/306 | 351/309 | 351/310 | 349/313 |
| SP-F | 338 | 343 | 341 | 338 | 341 | 342 | 340 |
| SP-Cl | 338 | 343 | 341 | 338 | 341 | 342 | 340 |
| SP-Br | 338 | 343 | 341 | 338 | 341 | 342 | 340 |
| SP-CN | 332 | 335 | 332 | 330 | 334 | 335 | 332 |
| SP-$NO_2$ | 329 | 331 | 330 | 327 | 331 | 333 | 327 |

**Table S2.** Fluorescence emission wavelengths of SP-OH derivatives in different solvents

| Dyes | THF | EtOH | MeOH | ACN | DMF | DMSO | $H_2O$ |
|---|---|---|---|---|---|---|---|
| SP-OH | 515 | 517 | 528 | 514 | 544 | 547 | 437/525 |
| SP-OH-Br | 524 | 531 | 538 | 527 | 574 | 569 | 449/539 |
| SP-OH-Cl | 524 | 531 | 538 | 525 | 574 | 568 | 449/543 |
| SP-OH-F | 524 | 538 | 543 | 527 | 566 | 569 | 437/536 |
| SP-OH-CN | 675 | 642 | 646 | 661 | 666 | 661 | 624 |
| SP-OH-$NO_2$ | 667 | 640 | 639 | 654 | 646 | 638 | 609 |
| SQ-OH-$NO_2$ | 725 | 689 | 689 | 705 | 717 | 711 | 670 |
| SP-OH-N | 589 | 600 | 601 | 608 | 605 | 608 | 606 |
| SP-OMe-$NO_2$ | 460 | 458 | 466 | 469 | 462 | 471 | 466 |
| SP-F | 332 | 410 | 416 | 420 | 336 | 415 | 422 |
| SP-Cl | 332 | 410 | 416 | 420 | 336 | 416 | 423 |
| SP-Br | 332 | 412 | 416 | 423 | 336 | 416 | 424 |
| SP-CN | 350 | 397 | 400 | 409 | 338 | 403 | 406 |
| SP-$NO_2$ | 355 | 394 | 395 | 396 | 338 | 365 | 399 |

## 3. **Density functional theory (DFT) calculations**

The ground-states of all structures were optimized at the B3LYP/6-31+G(d) level. The time-dependent density functional theory (TD-DFT) calculation used the CAM-B3LYP/6-31+G(d) method based on their optimized $S_0$ geometries. All the calculations were performed by Gaussian[1-10]. The natural transition orbit analysis was made using Multiwfn 3.8 based on the TD-DFT results.

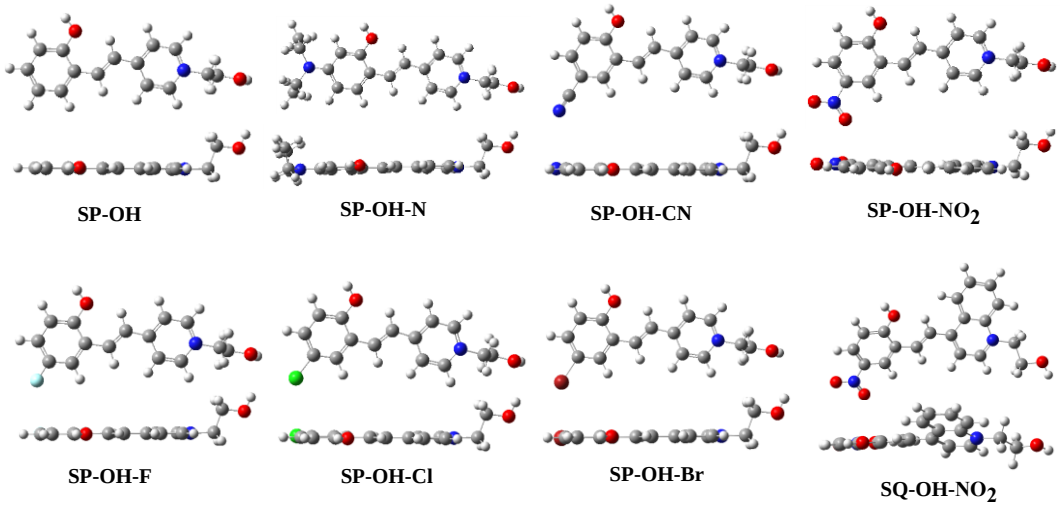


**Figure S14.** Molecular configurations of optimized SP-OH derivatives and SQ-OH-$NO_2$ at different angles.

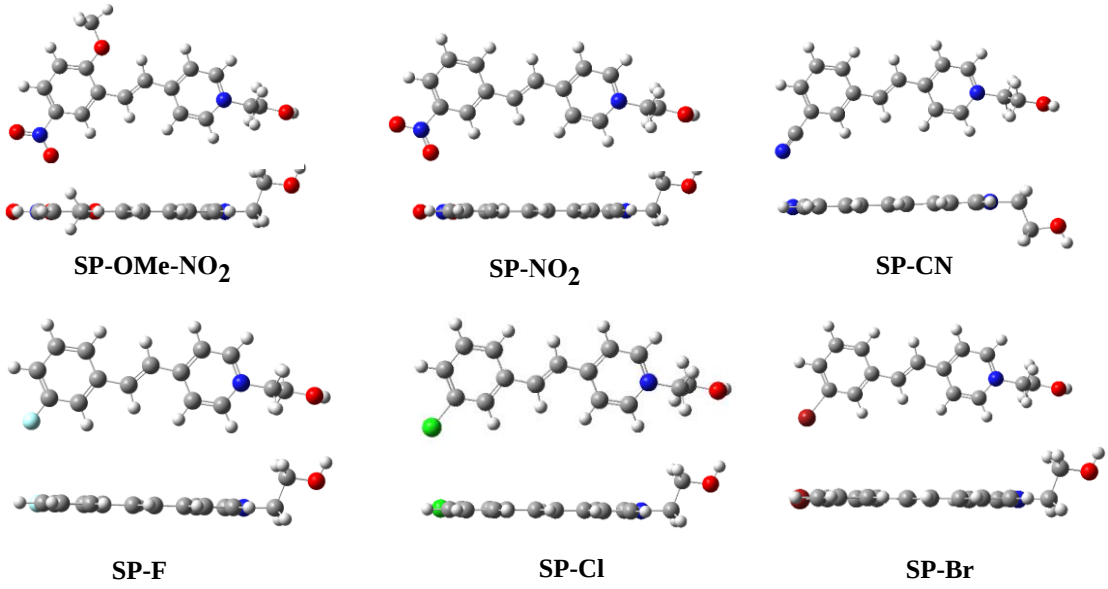


**Figure S15.** Molecular configurations of optimized SP derivatives and SP-OMe-$NO_2$ at different angles.

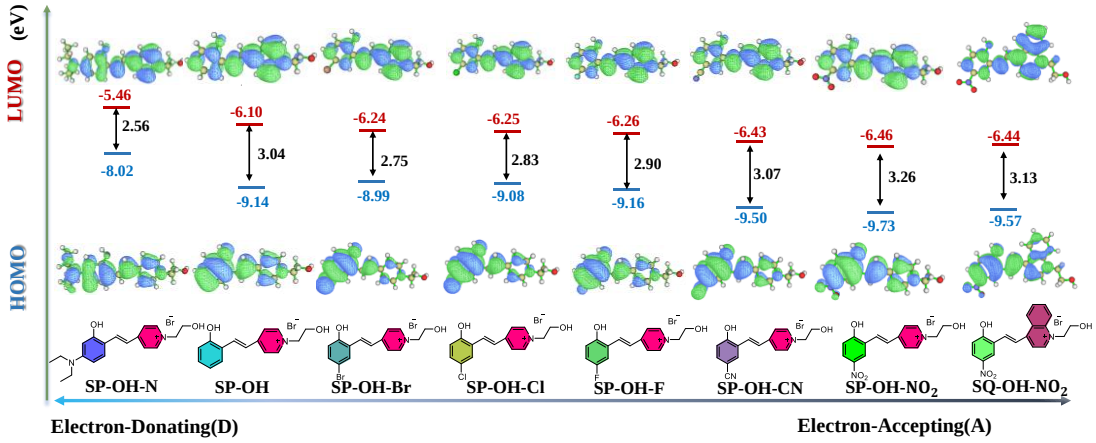


**Figure S16.** HOMO-LUMO energy levels and Molecular orbitals of compounds SP-OH derivatives and SQ-OH-$NO_2$.

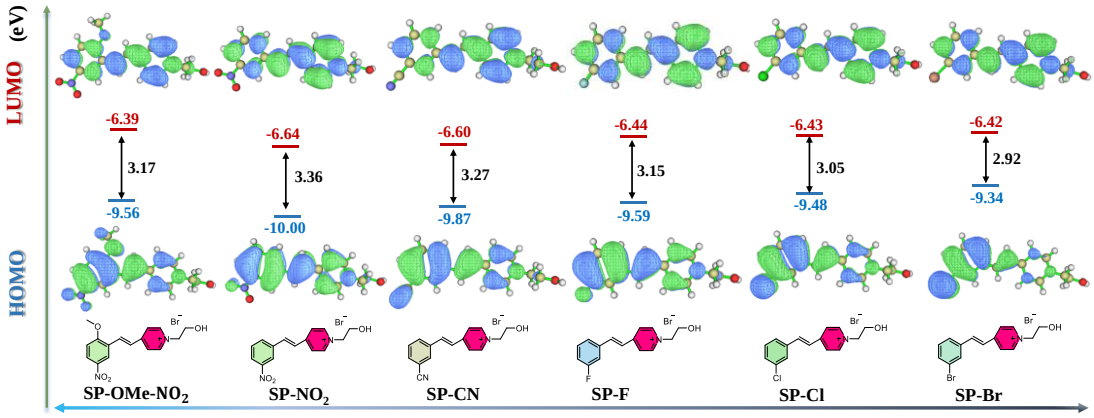


**Figure S17.** HOMO-LUMO energy levels and Molecular orbitals of compounds SP derivatives and SP-OMe-$NO_2$.

## 4. Syntheses and characterization

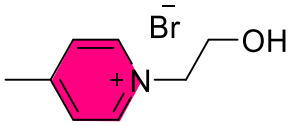


1-(2-hydroxyethyl)-4-methyl-pyridinium bromide

**4.1 Compound 1-(2-hydroxyethyl)-4-methyl-pyridinium bromide**:

4-methylpyridine (5 g, 53.76 mmol) and 2-bromoethanol (6.67 g, 53.76 mmol ) were added into a dry single-mouth flask, then anhydrous acetonitrile was added to stir and dissolve, and the reaction was continued at 80 ℃ for 16 h. After the reaction, the reaction solution was dried to obtain the crude product, which was directly used for the next reaction without purification. The prouduct was obtained as yellow oily substance (9.8g, yield: 83.62%). **$^1$H NMR** (400 MHz, 298 K, DMSO-d6) δ 8.91 (d, J=5.2 Hz, 2H), 8.01 (d, J=6.3Hz, 2H), 5.23 (s, 1H), 4.63 (t, J=4.0Hz, 2H), 3.82 (t, J=4.6Hz, 2H), 2.60 (s, 3H) ppm; **$^{13}$C NMR** (100 MHz, 298 K, DMSO-d6) δ 156.78, 142.08, 125.94, 60.04, 57.97, 19.46 ppm;

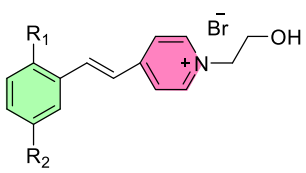


**SP-OH:** $R_1$=OH, $R_2$=H
**SP-OH-Br:** $R_1$=OH, $R_2$=Br
**SP-OH-Cl:** $R_1$=OH, $R_2$=Cl
**SP-OH-F:** $R_1$=OH, $R_2$=F
**SP-OH-CN:** $R_1$=OH, $R_2$=CN
**SP-OH-$NO_2$:** $R_1$=OH, $R_2$=$NO_2$
**SP-Br:** $R_1$=H, $R_2$=Br
**SP-Cl:** $R_1$=H, $R_2$=Cl
**SP-F:** $R_1$=H, $R_2$=F
**SP-CN:** $R_1$=H, $R_2$=CN
**SP-$NO_2$:** $R_1$=H, $R_2$=$NO_2$
**SP-OMe-$NO_2$:** $R_1$=$OCH_3$, $R_2$=$NO_2$

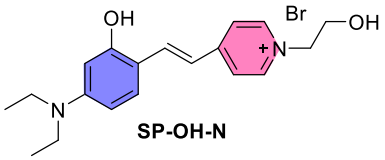


**SP-OH-N**

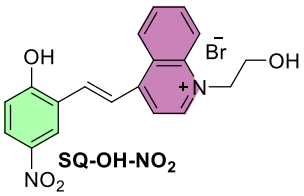


**SQ-OH-$NO_2$**

**4.2 General procedure for the synthesis of styryl-pyridinium derivatives:**

1-(2-hydroxyethyl)-4-methyl-pyridinium bromide (500 mg, 2.59 mmol) and 2-hydroxy-benzaldehyde derivatives (2.59 mmol) were mixed in 20 mL absolute ethanol. The mixture was heated at 80 °C and maintained with

continuously stirring for 10min, then added amine acetate (50 mg) at this temperature and continued stirring for 10 h. Then the crude product was evaporated by a rotary evaporator to remove redundant ethanol and followed by silica-gel column chromatography ($CH_2Cl_2$/$CH_3OH$, 5:1, v/v) or recrystallization to afford the probe styryl-pyridinium derivatives.

**Compound SP-OH** was obtained as yellow solid (880 mg, yield: 91.40%). **$^1$H NMR** (400 MHz, 298 K, DMSO-d6) δ 10.36 (s, 1H)，8.83 (d, J=7.2 Hz, 2H), 8.23 (d, J=6.8 Hz, 2H), 8.06 (d, J=16.4 Hz, 1H), 7.69 (d, J=7.8 Hz, 1H), 7.55 (d, J=16.4 Hz, 1H), 7.28 (t, J=7.8 Hz, 1H), 6.99 (d, J=8.1 Hz, 1H), 6.91 (t, J=7.6 Hz, 1H), 5.25 (s, 1H), 4.56 (t, J=4.9 Hz, 2H), 3.85 (t, J=4.6 Hz, 2H) ppm; **$^{13}$C NMR** (100 MHz, 298 K, DMSO-d6) δ 157.37, 154.01, 145.00, 137.04, 132.27, 129.26, 126.44, 123.70, 123.32, 122.34, 120.04, 116.83, 62.38, 60.53 ppm;

**Compound SP-OH-Br** was obtained as yellow solid (639 mg, yield: 64.25%). **$^1$H NMR** (400 MHz, 298 K, DMSO-d6) δ 10.71 (s, H), 8.84 (d, J=6.2 Hz, 2H), 8.24 (d, J=6.6 Hz, 2H), 7.97 (d, J=16.4 Hz, 1H), 7.88 (t, t=2.2 Hz, 1H), 7.63 (d, J=16.5 Hz, 1H), 7.41 (dt, J=8.8, 1.9 Hz, 1H), 6.95 (dt, J=8.8, 1.0 Hz, 1H), 4,56 (t, J=4.8 Hz, 2H), 3.84 (t, J=4.8 Hz, 2H) ppm; **$^{13}$C NMR** (100 MHz, 298 K, DMSO-d6) δ 162.13, 156.28, 145.16, 134.33, 130.99, 123.98, 119.59, 118.86, 111.62, 102.67, 100.41, 94.04, 62.53, 55.44 ppm;

**Compound SP-OH-Cl** was obtained as yellow solid (863 mg, yield: 75.63%) **$^1$H NMR** (400 MHz, 298 K, DMSO-d6) δ 10.68 (s, 1H), 8.86 (d, J=6.9 Hz, 2H), 8.22 (d, J=6.8 Hz, 2H), 7.98 (d, J=16.5 Hz, 1H), 7.77 (d, J=2.6 Hz, 1H), 7.63 (d, J=16.4 Hz, 1H), 7.30 (dd, J=8.7, 2.6 Hz, 1H), 7.00 (d, J=8.7 Hz, 1H), 5.25 (t, J=5.2 Hz, 1H), 4.57 (t, J=5.0 Hz, 2H), 3.86 (q, J=4.7 Hz, 2H) ppm; **$^{13}$C NMR** (100 MHz, 298 K, DMSO-d6) δ 156.04, 153.55, 145.13, 142.75, 135.15, 131.50, 128.04, 124.72, 124.05, 123.96, 123.68, 62.53, 60.50 ppm;

**Compound SP-OH-F** was obtained as yellow solid (674 mg, yield: 55.53%). **$^1$H NMR** (400 MHz, 298 K, DMSO-d6) δ 10.37 (s, 1H), 8.85 (t, J=4.2 Hz, 2H), 8.23 (d, J=6.3 Hz, 2H), 8.00 (d, J=16.4 Hz, 1H), 7.56 (m, 2H), 7.14 (td, J=8.5, 2.0 Hz, 1H), 6.97 (m, 1H), 5.25 (t, J=5.0 Hz, 1H), 4.57 (d, J=3.0 Hz, 2H), 3.85 (q, J=10.1, 4.6 Hz, 2H) ppm; **$^{13}$C NMR** (100 MHz, 298 K, DMSO-d6) δ 153.60, 153.53, 145.15, 136.42, 136.13, 135.42, 124.54, 123.93, 118.87, 117.87, 114.12, 62.51, 60.51 ppm;

**Compound SP-OH-CN** was obtained as orange solid (37 mg, yield: 31.36%). **$^1$H NMR** (400 MHz, 298 K, DMSO-d6) δ 11.57 (s, 1H), 8.87 (d, J=6.4 Hz, 2H), 8.25 (d, J=6.3 Hz, 2H), 8.20 (d, J=2.0 Hz, 1H), 7.99 (d, J=16.5 Hz, 1H), 7.69(m, 2H), 7.10 (dd, J=8.6, 2.5 Hz, 1H), 5.25 (t, J=5.1 Hz, 1H), 4.58 (t, J=4.5 Hz, 2H), 3.86 (q, J=5.0 Hz, 2H) ppm; **$^{13}$C NMR** (100 MHz, 298 K, DMSO-d6) δ 160.80, 145.26, 135.37, 134.37, 133.37, 125.66, 124.13, 123.66, 119.47, 117.82, 102.37 ppm;

**Compound SP-OH-$NO_2$** was obtained as bright red solid (758 mg, yield: 69.08%). **$^1$H NMR** (400 MHz, 298 K, DMSO-d6) δ 10.17 (s, 1H), 8.79 (d, J=6.9 Hz, 2H), 8.46 (d, J=3.0 Hz, 1H), 8.19 (d, J=6.7 Hz, 2H), 8.00 (m, 2H), 7.86 (d, J=16.3 Hz, 1H), 6.74 (d, J=9.7 Hz, 1H), 4.52 (t, J=4.7 Hz, 2H), 3.84 (t, J=4.8 Hz, 2H) ppm; **$^{13}$C NMR**

(100 MHz, 298 K, DMSO-d6) δ 154.34, 144.82, 137.83, 135.91, 130.20, 127.39, 123.47, 122.83, 119.64, 62.32, 60.51 ppm;

**Compound SP-OH-OMe** was obtained as orange solid (486 mg, yield: 59.73%). **$^{1}$H NMR** (400 MHz, 298 K, DMSO-d6) δ 9.98 (s, 1H), 8.84 (d, J=6.3 Hz, 2H), 8.21 (d, J=5.9 Hz, 2H), 8.04 (d, J=16.4 Hz, 1H), 7.54 (d, J=7.5 Hz, 2H), 7.26 (s, 1H), 6.90 (m, 2H), 5.26 (t, J=9.51 Hz, 1H), 4.56 (t, J=8.6 Hz, 2H), 3.85 (dd, J=3.9 14.2 Hz, 2H), 3.75 (s, 3H) ppm; **$^{13}$C NMR** (100 MHz, 298 K, DMSO-d6) δ 153.94, 152.81, 151.58, 145.00, 136.70, 123.68, 123.40, 122.51, 119.18, 117.75, 112.31, 62.41, 60.51, 56.06 ppm;

**Compound SP-OH-*m*-NO$_2$** was obtained as dark red solid (654 mg, yield: 64.56%). **$^{1}$H NMR** (400 MHz, 298 K, DMSO-d6) δ 11.38 (s, 1H), 8.91 (d, J=5.6 Hz, 2H), 8.33 (d, J=6.6 Hz, 2H), 8.06 (d, J=16.4 Hz, 1H), 7.93 (d, J=8.9 Hz, 1H), 7.78 (m, 2H), 7.74 (s, 1H), 5.24 (t, J=8.8 Hz, 1H), 4.58 (t, J=7.0 Hz, 2H), 3.86 (m, 2H) ppm; **$^{13}$C NMR** (100 MHz, 298 K, DMSO-d6) δ 157.33, 153.07, 148.96, 145.34, 134.45, 130.12, 129.04, 128.42, 127.54, 124.47, 114.71, 111.04, 62.72, 60.51 ppm;

**Compound SP-Br** was obtained as light yellow solid (254 mg, yield: 24.43%). **$^{1}$H NMR** (400 MHz, 298 K, DMSO-d6) δ 8.93 (d, J=6.6 Hz, 2H), 8.25 (d, J=6.5 Hz, 2H), 8.01 (t, J=8.1 Hz, 2H), 7.74 (d, J=7.8 Hz, 1H), 7.64 (t, J=6.5 Hz, 2H), 7.46 (d, J=8.0 Hz, 1H), 5.26 (t, J=5.2 Hz, 1H), 4.59 (t, J=4.4 Hz, 2H), 3.87 (q, J=5.3 Hz, 2H) ppm; **$^{13}$C NMR** (100 MHz, 298 K, DMSO-d6) δ 152.97, 145.39, 139.30, 138.12, 133.24, 131.70, 130.65, 127.79, 125.44, 124.25, 122.93, 62.72, 60.49 ppm;

**Compound SP-Cl** was obtained as light yellow solid (589 mg, yield: 48.53%). **$^{1}$H NMR** (400 MHz, 298 K, DMSO-d6) δ 8.92 (d, J=6.9 Hz, 2H), 8.26 (d, J=6.9 Hz, 2H), 7.99 (d, J=16.4 Hz, 1H), 7.87 (s, 1H), 7.68 (m, 2H), 7.52 (m, 2H), 5.24 (t, J=5.4 Hz, 1H), 4.58 (t, J=4.8 Hz, 2H), 3.87 (q, J=5.3 Hz, 2H) ppm; **$^{13}$C NMR** (100 MHz, 298 K, DMSO-d6) δ 152.94, 145.40, 139.36, 137.87, 134.35, 131.45, 130.36, 127.72, 127.46, 125.47, 124.25, 62.73, 60.49 ppm;

**Compound SP-F** was obtained as light yellow solid (142 mg, yield: 10.87%). **$^{1}$H NMR** (400 MHz, 298 K, DMSO-d6) δ 8.93 (m, 2H), 8.26 (m, 2H), 8.00 (d, J=15.6 Hz, 1H), 7.57 (m, 4H), 7.31 (m, 1H), 4.58 (s, 2H), 3.85 (t, J=4.8 Hz, 2H) ppm; **$^{13}$C NMR** (100 MHz, 298 K, DMSO-d6) δ 163.93, 161.99, 152.98, 145.37, 139.63, 138.17, 131.56, 125.37, 125.23, 124.24, 117.57, 114.45, 62.66, 60.49 ppm;

**Compound SP-CN** was obtained as light yellow solid (272 mg, yield: 21.51%). **$^{1}$H NMR** (400 MHz, 298 K, DMSO-d6) δ 8.95 (d, J=6.5 Hz, 2H), 8.28 (d, J=6.3 Hz, 2H), 8.03 (m, 1H), 7.67 (m, 3H), 7.52 (m, 1H), 7.29 (t, J=8.5, 16.7 Hz, 1H), 5.25 (t, J=5.3, 10.74 Hz, 1H), 4.60 (t, J=4.3, 5.2, 9.0 Hz, 2H), 3.86 (q, J=4.5, 5.1, 10.1 Hz, 2H) ppm; **$^{13}$C NMR** (100 MHz, 298 K, DMSO-d6) δ 164.18, 161.76, 153.02, 145.34, 139.66, 138.16, 131.59, 125.38, 125.17, 124.26, 117.55, 114.49, 62.69, 60.48 ppm;

**Compound SP-NO$_2$** was obtained as light yellow solid (458 mg, yield: 39.45%). **$^{1}$H NMR** (400 MHz, 298 K,

DMSO-d6) δ 8.98 (d, J=6.5 Hz, 2H), 8.60 (t, J=4.7 Hz, 1H), 8.31 (m, 3H), 8.21 (m, 2H), 7.80 (m, 2H), 4.59 (t, J=4.7 Hz, 2H), 3.86 (t, J=4.8 Hz, 2H) ppm; **$^{13}$C NMR** (100 MHz, 298 K, DMSO-d6) δ 152.74, 148.86, 145.52, 138.54, 137.42, 134.54, 131.16, 126.56, 124.90, 124.45, 122.72, 62.82, 60.49 ppm;

**Compound SP-OH-N** was obtained as dark brown oily substance (643 mg, yield: 63.17%). **$^{1}$H NMR** (400 MHz, 298 K, $D_2O$) δ 8.23 (d, J=6.5 Hz, 2H), 8.19 (s, 1H), 7.74 (d, J=6.5 Hz, 2H), 7.56 (d, J=8.9 Hz, 1H), 6.94 (d, J=15.9 Hz, 1H), 6.33 (d, J=9.0 Hz, 1H), 6.07 (s, 1H), 4.42 (t, J=4.6 Hz, 2H), 4.03 (t, J=4.6 Hz, 2H), 3.41 (q, J=7.6 Hz, 4H), 1.20 (t, J=7.0 Hz, 6H) ppm; **$^{13}$C NMR** (100 MHz, 298 K, DMSO-d6) δ 159.74, 159.25, 154.91, 151.43, 144.60, 143.97, 138.45, 131.39, 128.42, 121.79, 116.32, 105.09, 62.66, 61.58, 60.53, 60.43, 44.47, 21.85, 13.09 ppm;

**Compound SP-OMe-$NO_2$** was obtained as yellow solid (876 mg, 83.59%). **$^{1}$H NMR** (400 MHz, 298 K, DMSO-d6) δ 8.91 (d, J=6.8 Hz, 2H), 8.64 (d, J=2.8 Hz, 1H), 8.34 (d, J=6.9 Hz, 3H), 8.09 (d, J=16.4 Hz, 1H), 7.79 (d, J=16.7 Hz, 1H), 7.37 (d, J=8.8 Hz, 1H), 5.26 (t, J=5.1 Hz, 1H), 4.59 (t, J=4.8 Hz, 2H), 4.07 (s, 3H), 3.86 (q, J=5.2 Hz, 2H) ppm; **$^{13}$C NMR** (100 MHz, 298 K, DMSO-d6) δ 162.99, 153.07, 145.38, 141.38, 133.81, 127.47, 127.17, 124.75, 124.44, 113.10, 62.72, 60.51, 57.52 ppm;

**Compound SQ-OH-$NO_2$** was obtained as black solid (954 mg, 88.04%). **$^{1}$H NMR** (400 MHz, 298 K, DMSO-d6) δ 9.07 (d, J=6.47 Hz, 1H), 8.85 (d, J=8.25 Hz, 1H), 8.79 (d, J=16.50 Hz, 1H), 8.65 (d, J=2.45 Hz, 1H), 8.50 (d, J=9.02 Hz, 1H), 8.39 (d, J=6.57 Hz, 1H), 8.2 (d, J=7.71 Hz, 1H), 8.16 (d, J=7.56 Hz, 1H), 8.02 (d, J=8.28 Hz, 1H), 7.98 (dd, J=9.58, 2.6 Hz, 1H), 6.68 (d, J=9.49 Hz, 1H), 5.01 (t, J=4.85 Hz, 2H), 2.01 (t, J=4.85 Hz, 2H) ppm; **$^{13}$C NMR** (100 MHz, 298 K, DMSO-d6) δ 164.42, 154.08, 148.46, 139.38, 138.51, 136.83, 135.16, 129.44, 127.58, 127.07, 126.91, 123.18, 119.70, 119.46, 115.93, 59.39, 59.16 ppm;

## 5. Supplemental Spectra

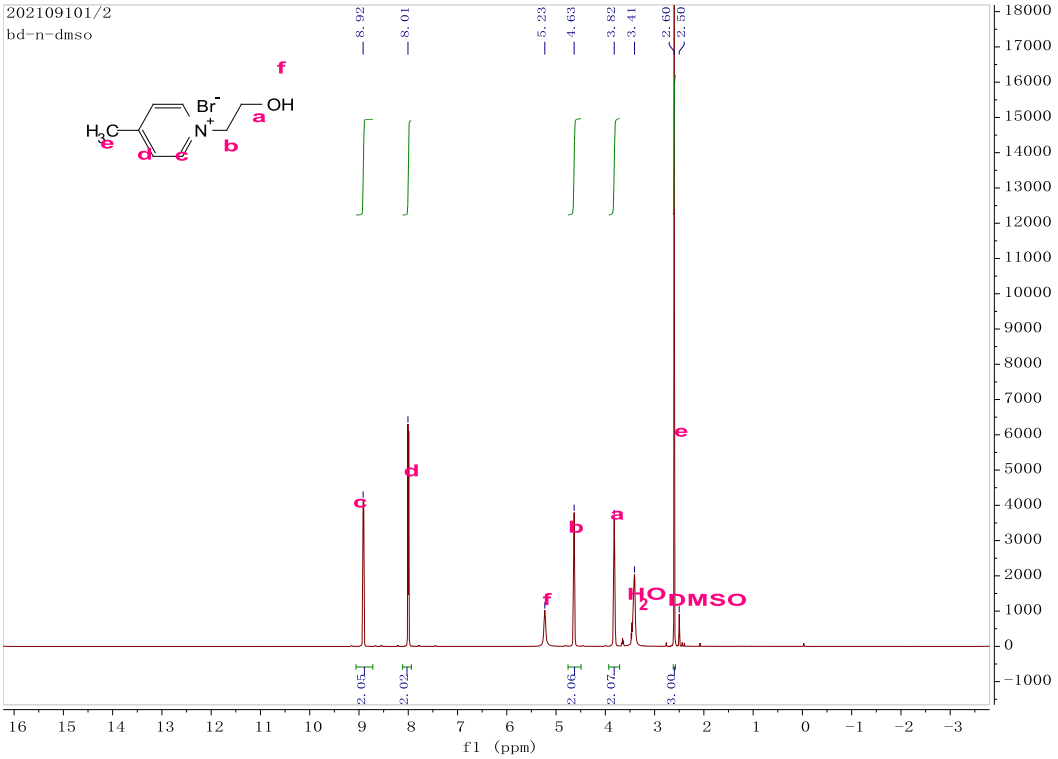


$^{1}$H NMR spectrum of 1-(2-hydroxyethyl)-4-methyl-pyridinium bromide

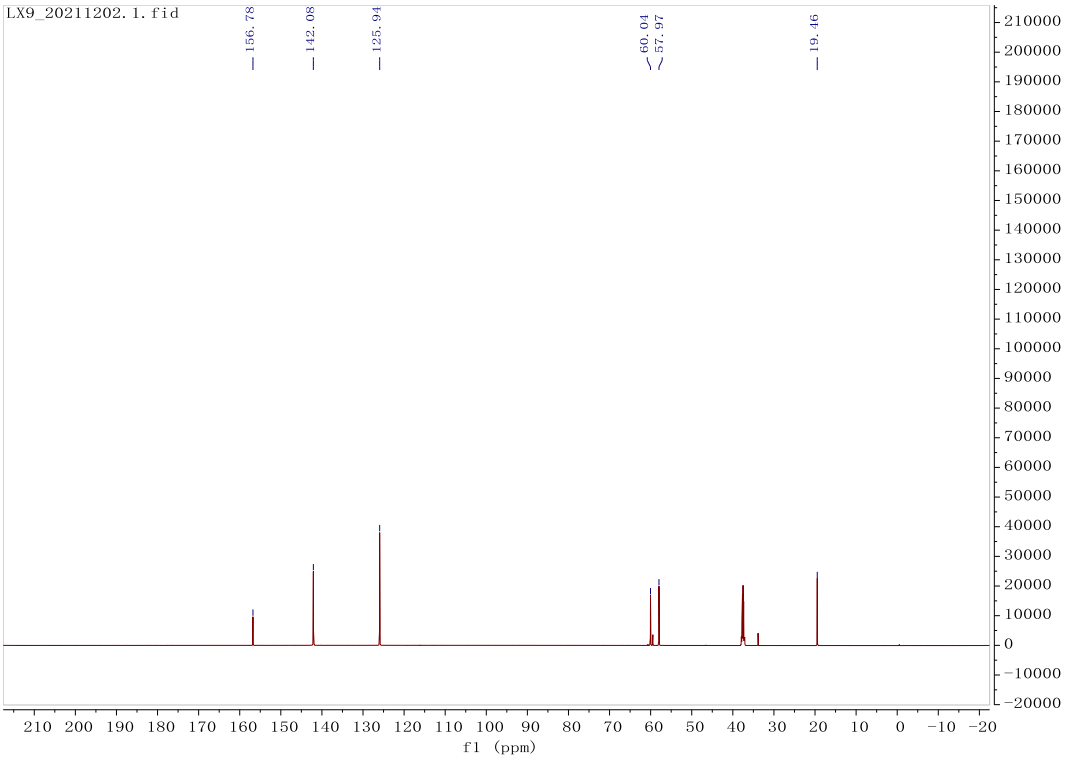


$^{13}$C NMR spectrum of 1-(2-hydroxyethyl)-4-methyl-pyridinium bromide

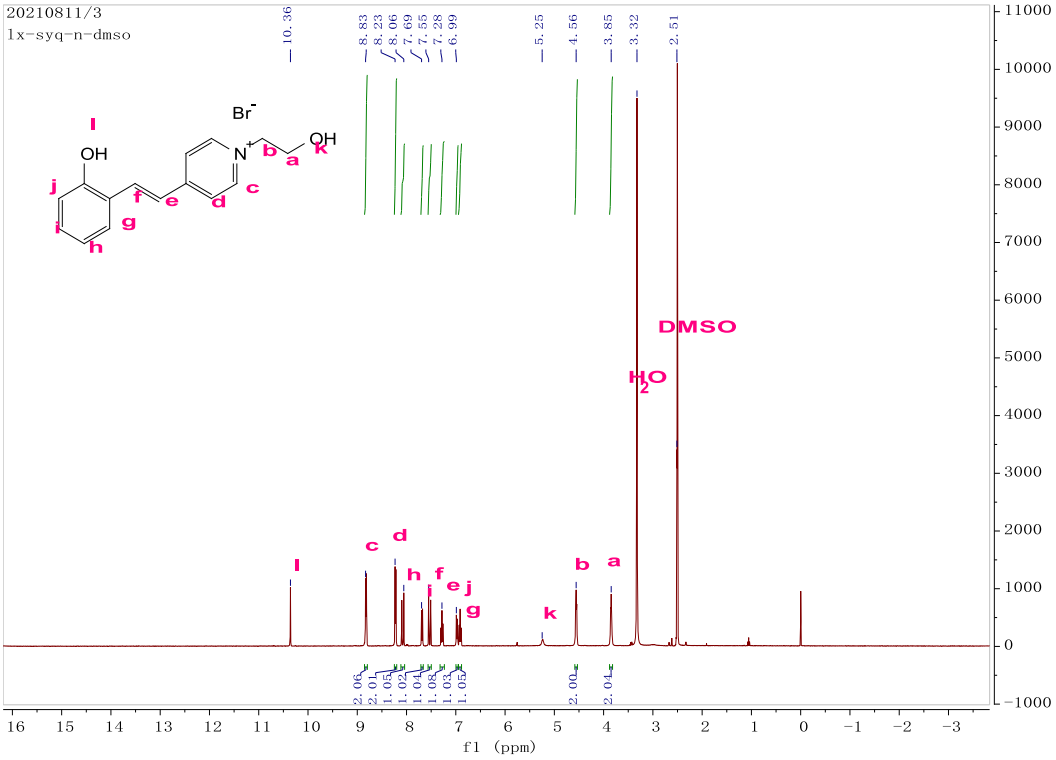


$^{1}$H NMR spectrum of SP-OH

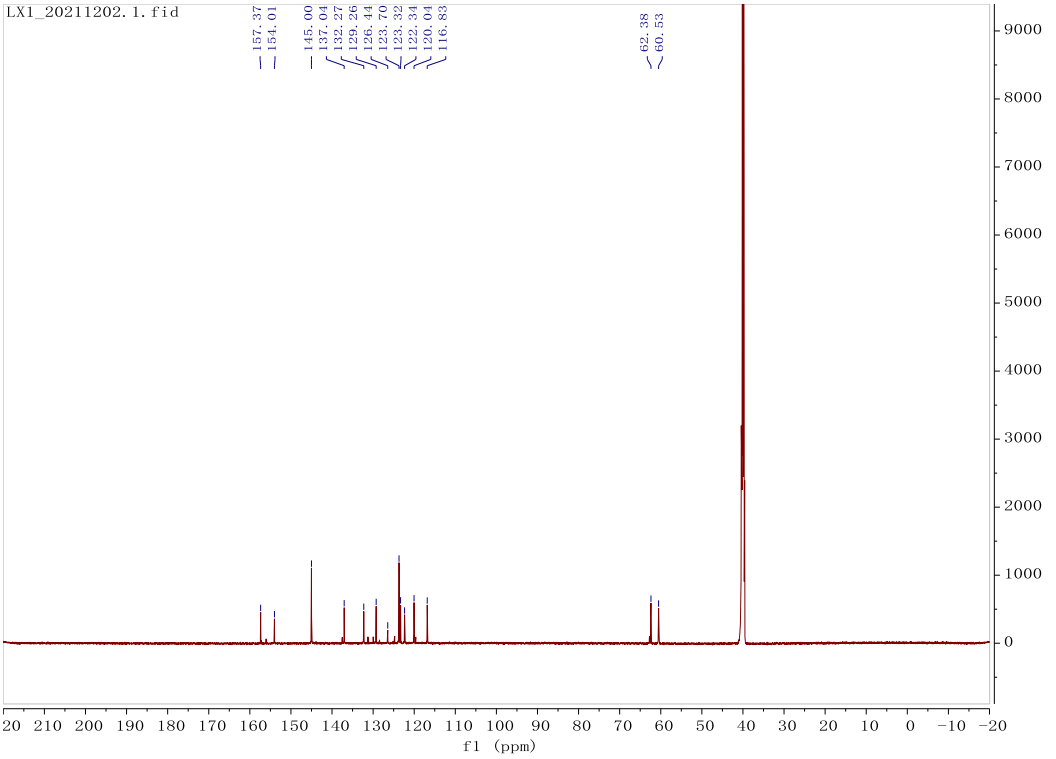


$^{13}$C NMR spectrum of SP-OH

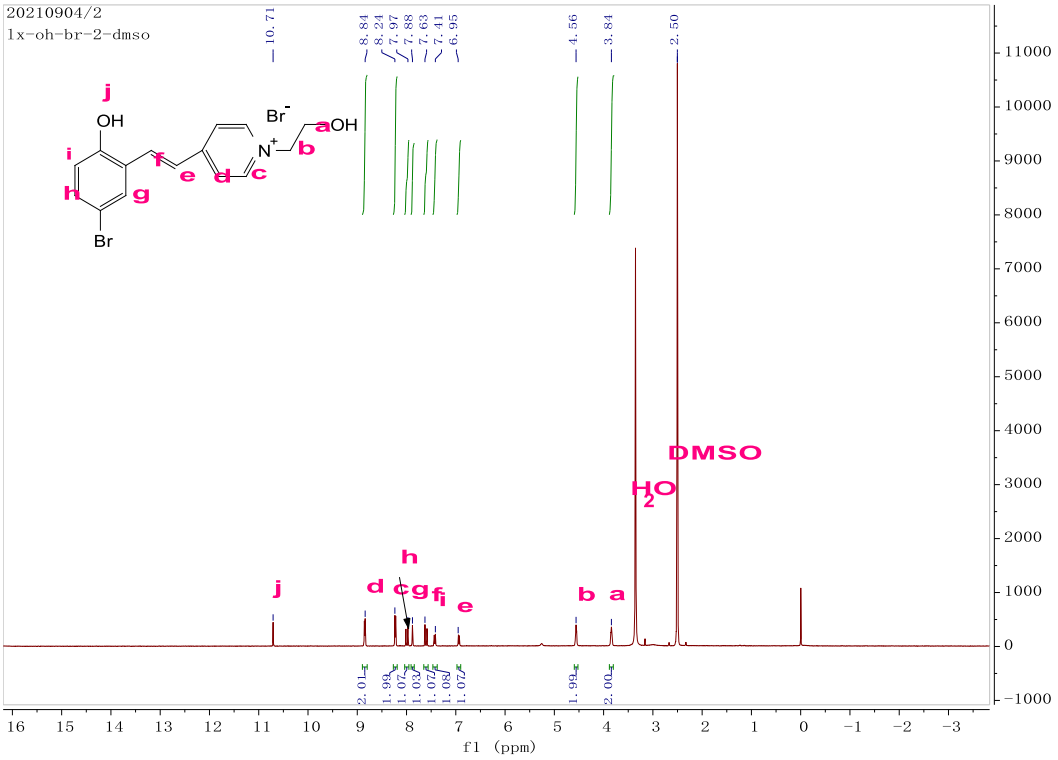


$^{1}$H NMR spectrum of SP-OH-Br

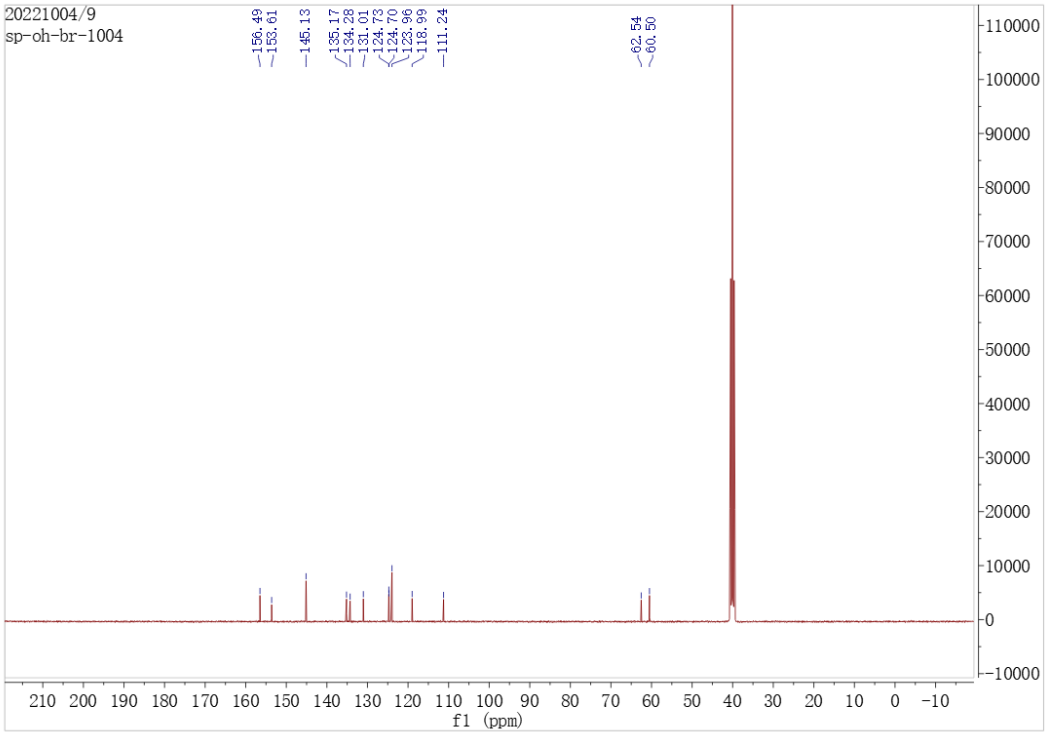


$^{13}$C NMR spectrum of SP-OH-Br

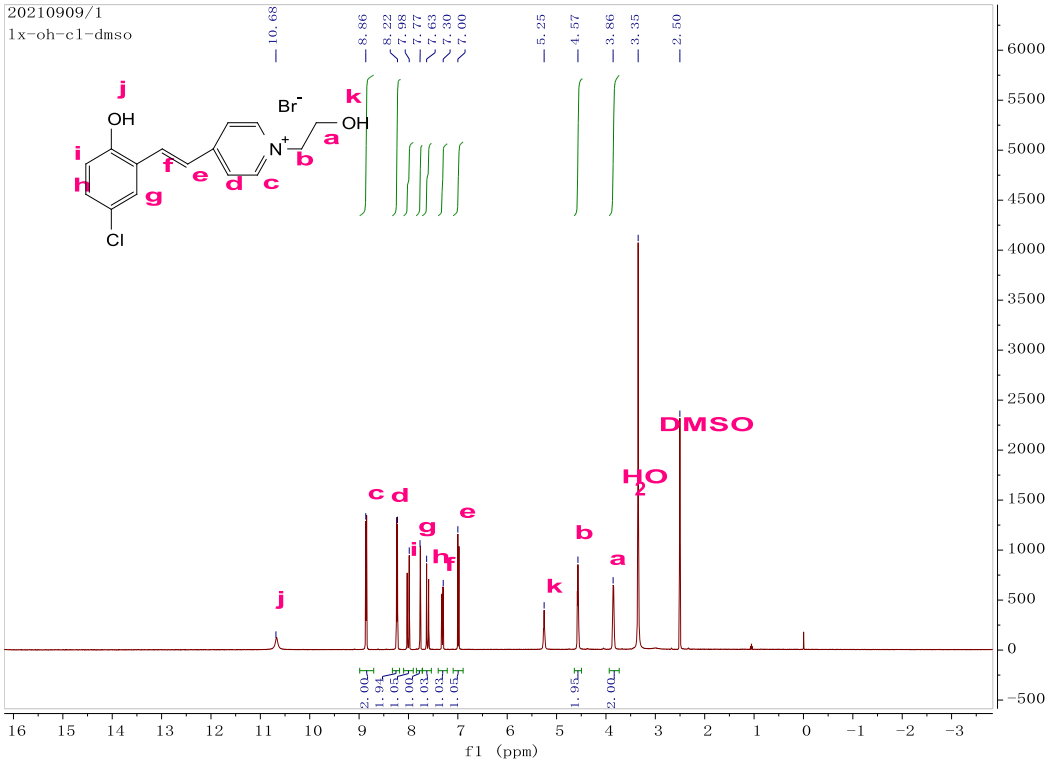


$^{1}$H NMR spectrum of SP-OH-Cl

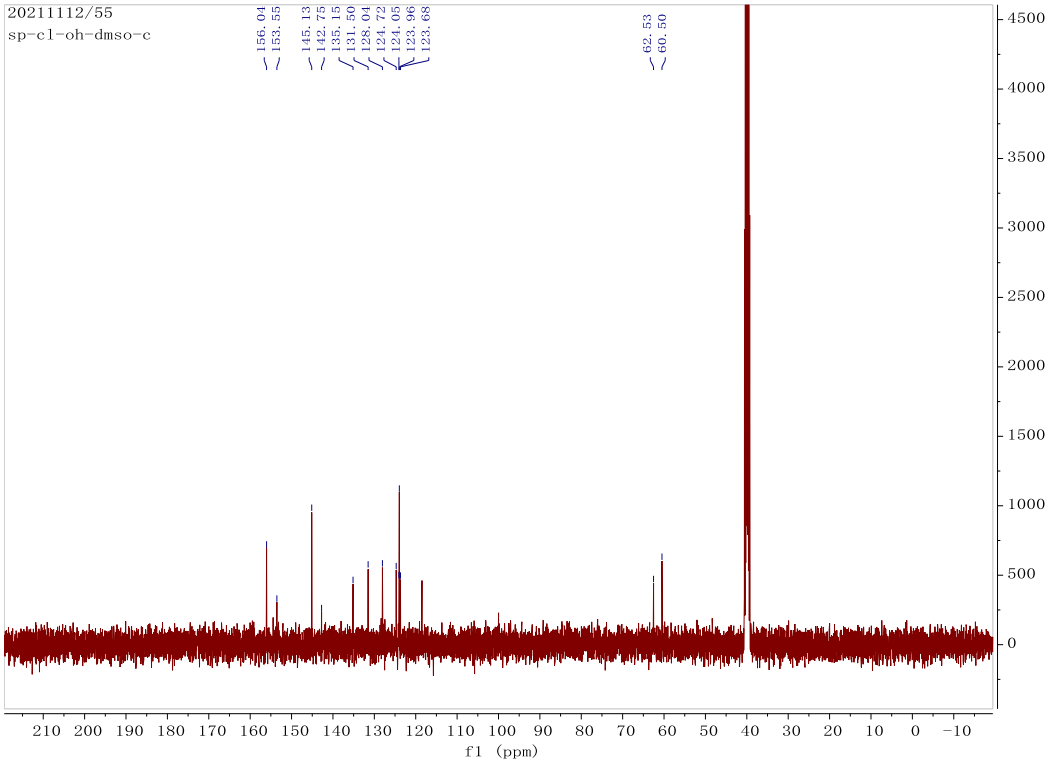


$^{13}$C NMR spectrum of SP-OH-Cl

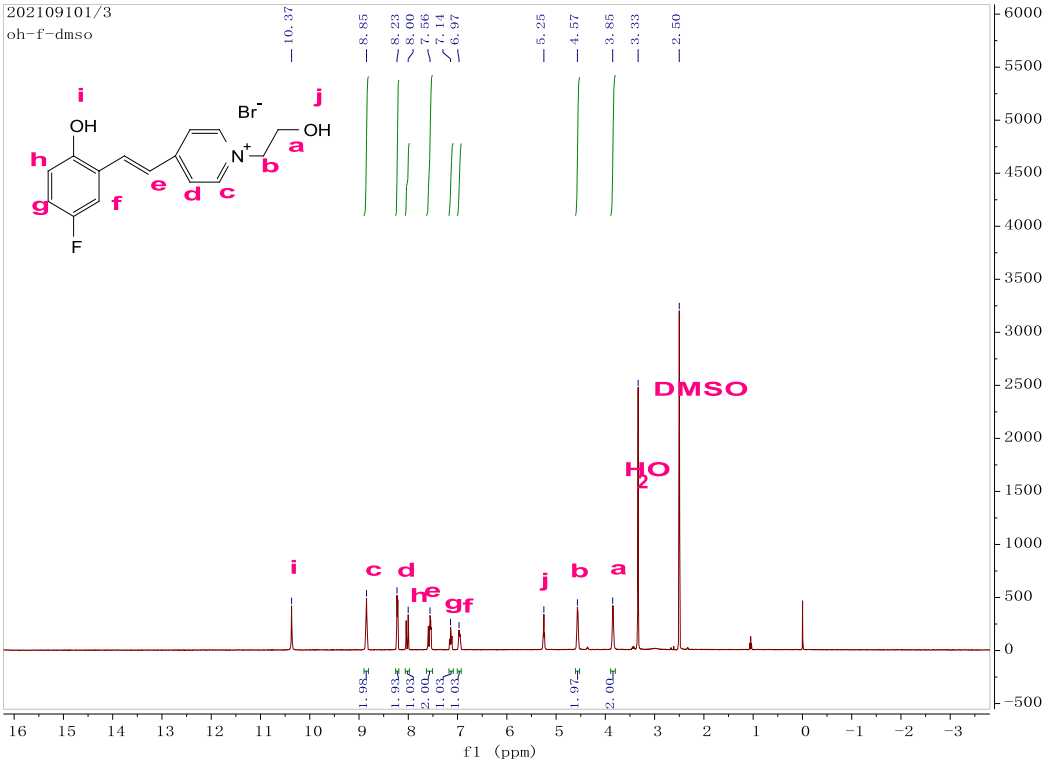


$^{1}$H NMR spectrum of SP-OH-F

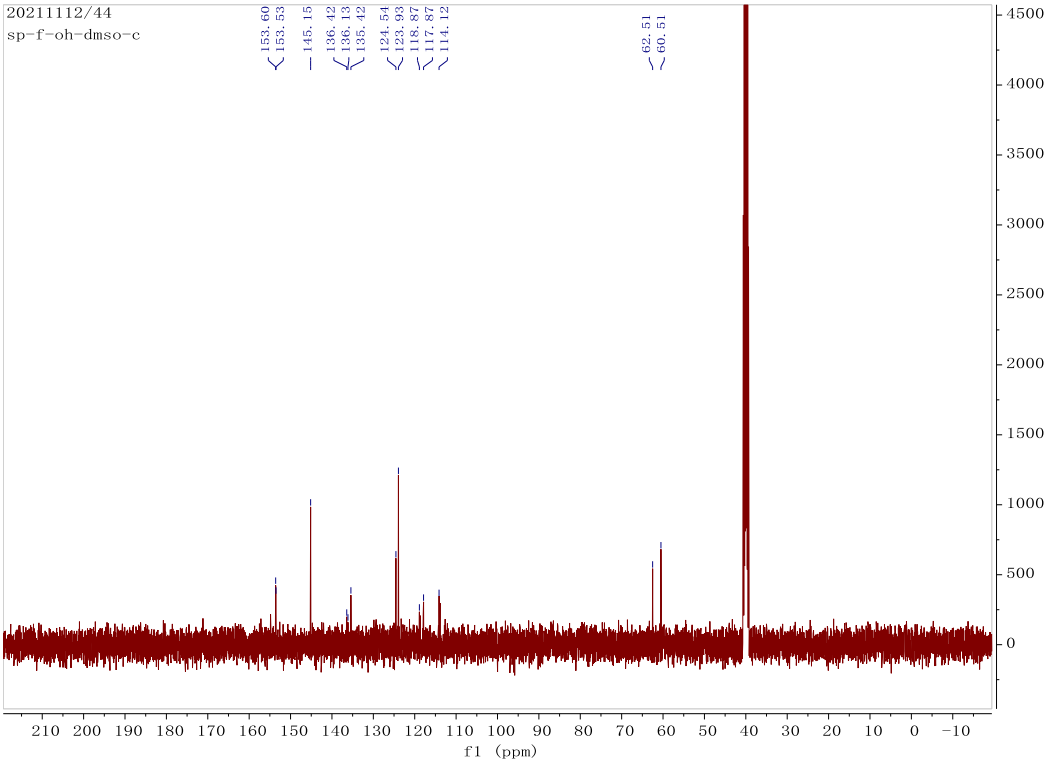


$^{13}$C NMR spectrum of SP-OH-F

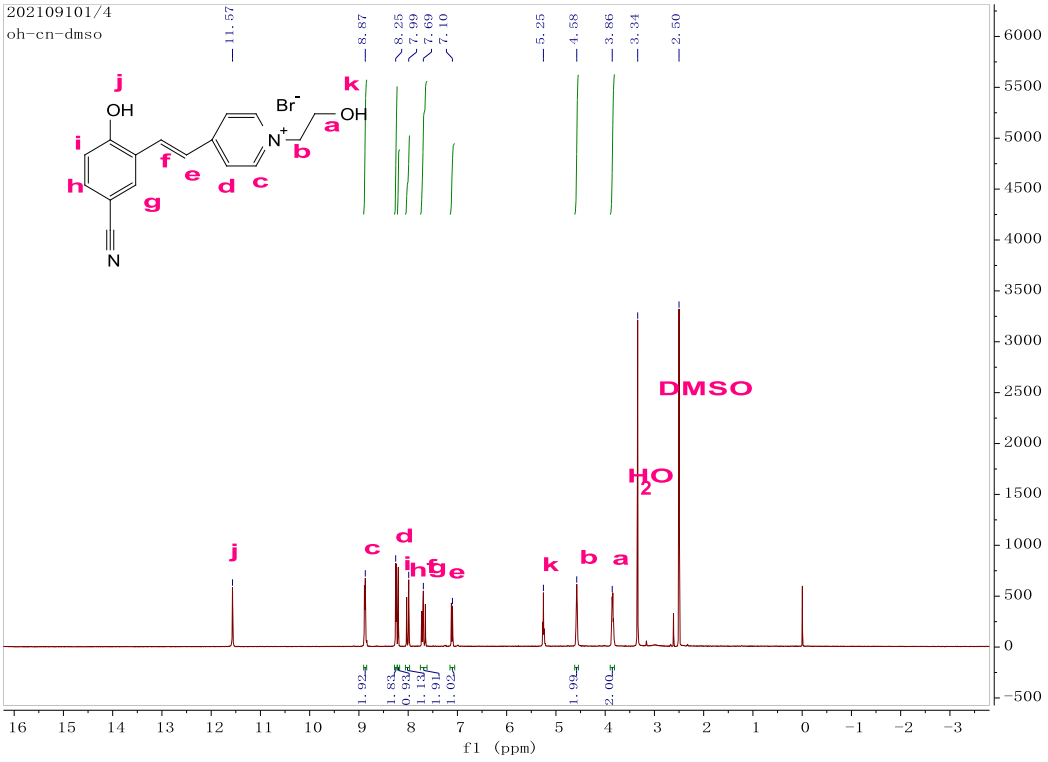


$^{1}$H NMR spectrum of SP-OH-CN

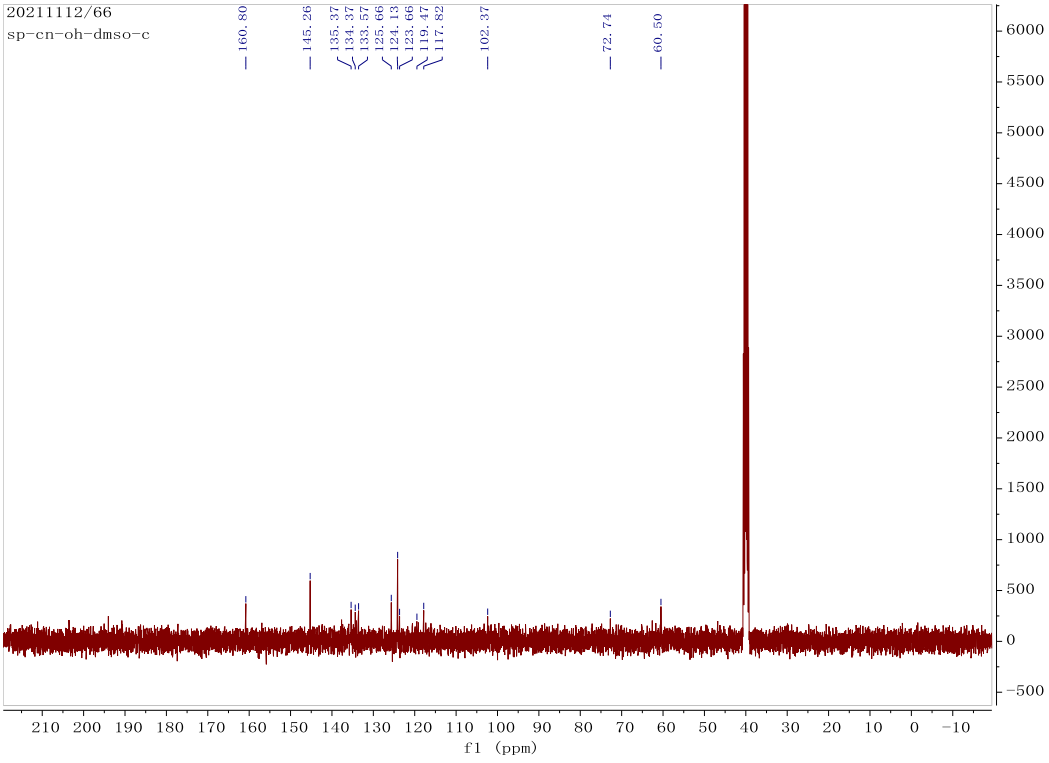


$^{13}$C NMR spectrum of SP-OH-CN

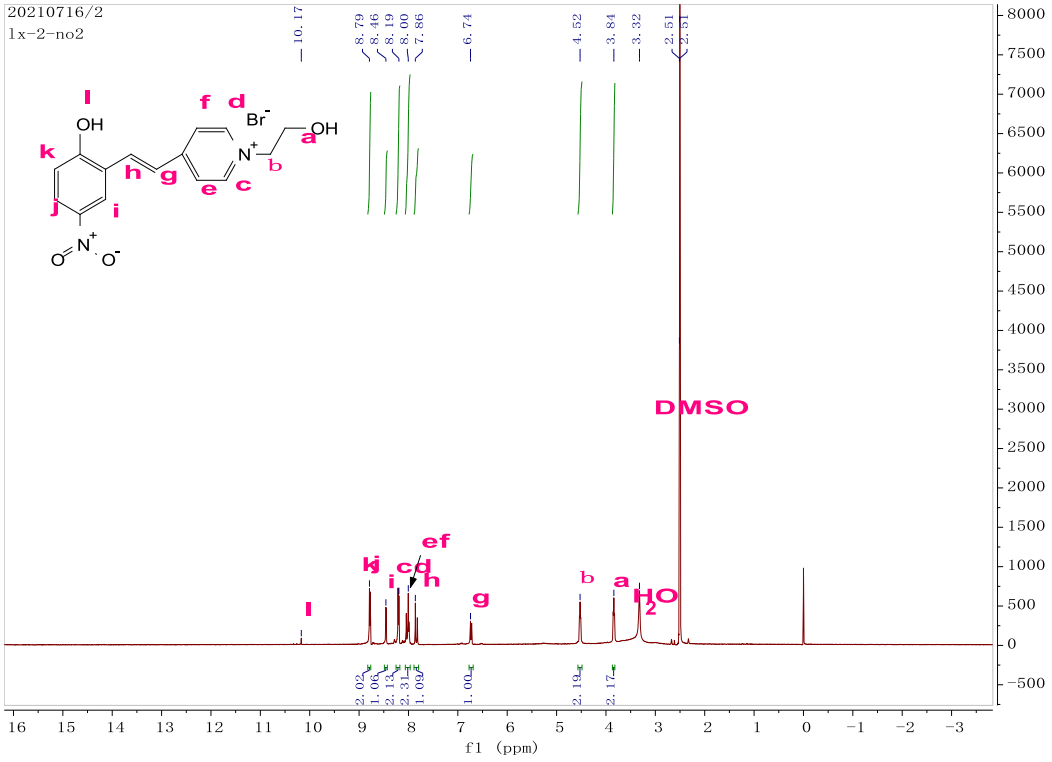


$^{1}$H NMR spectrum of SP-OH-NO$_2$

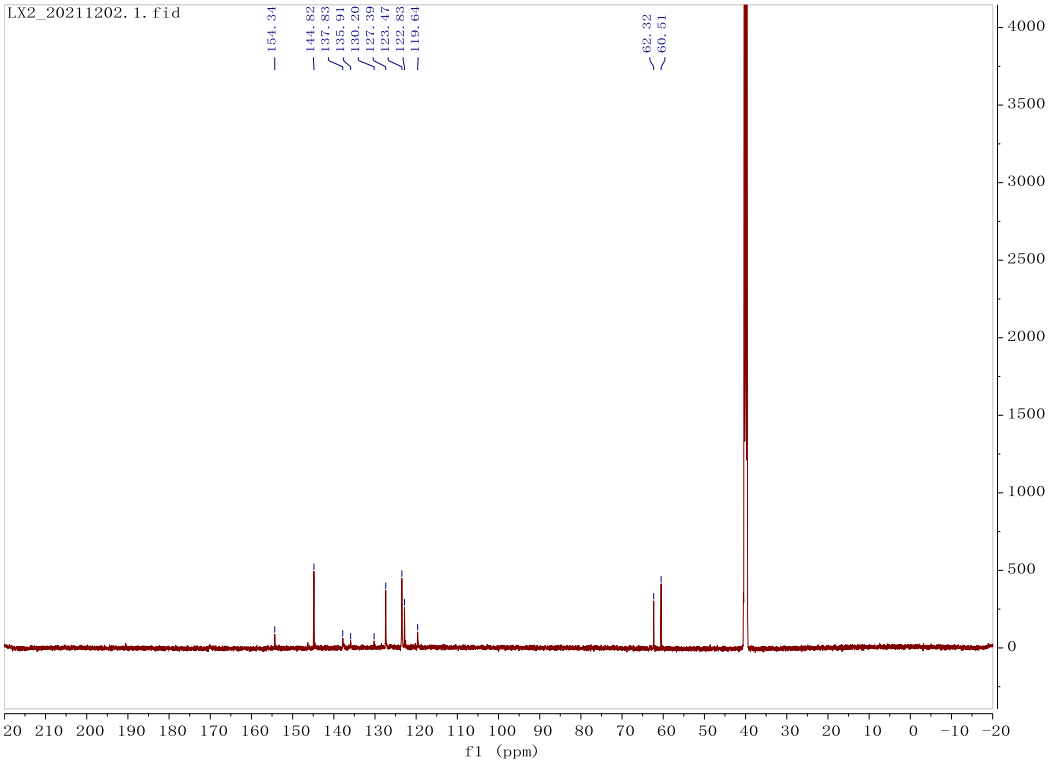


$^{13}$C NMR spectrum of SP-OH-NO$_2$

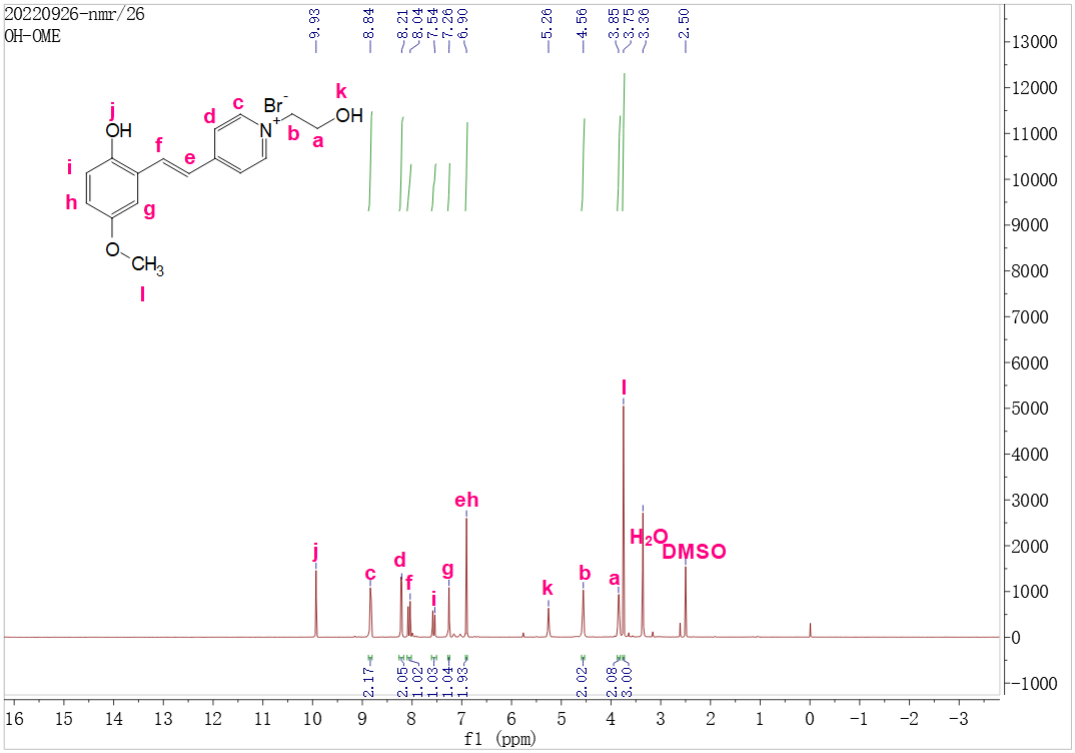


$^{1}$H NMR spectrum of SP-OH-OMe

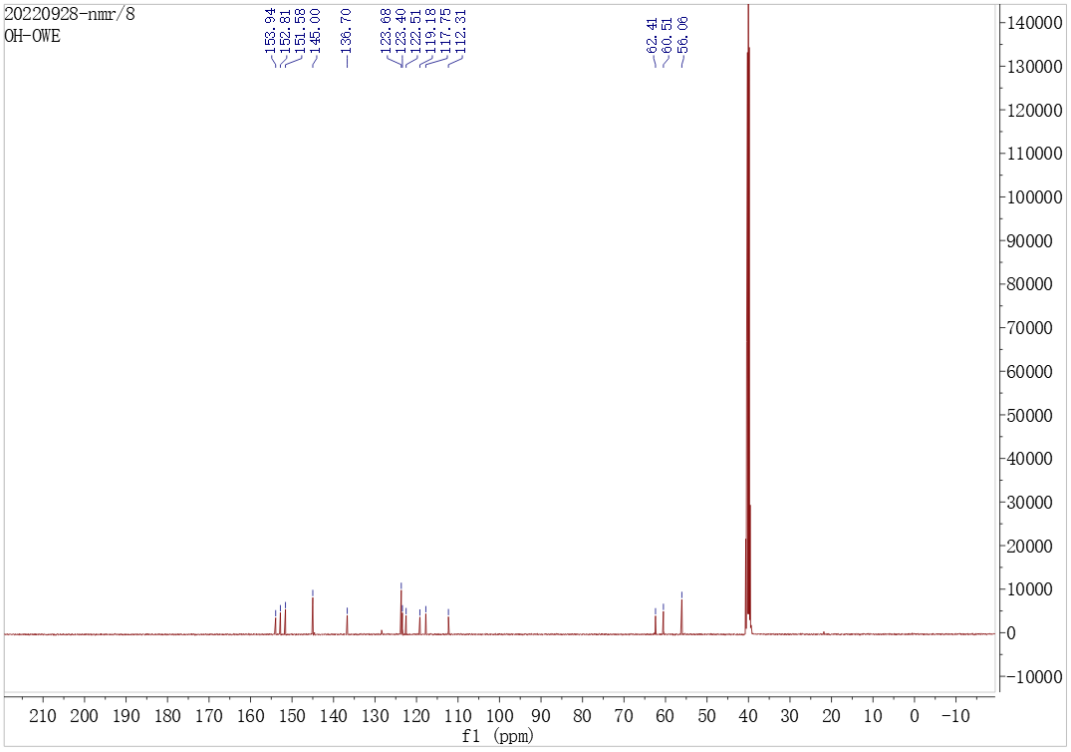


$^{13}$C NMR spectrum of SP-OH-OMe

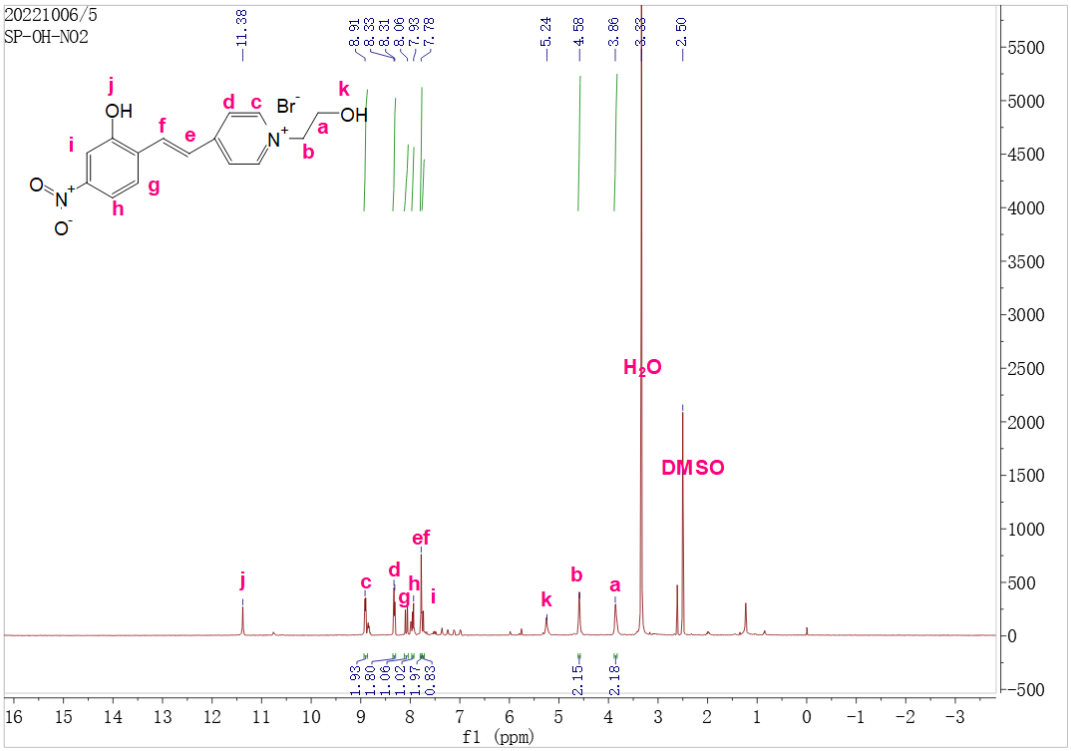


$^{1}$H NMR spectrum of SP-OH-*m*-$NO_2$

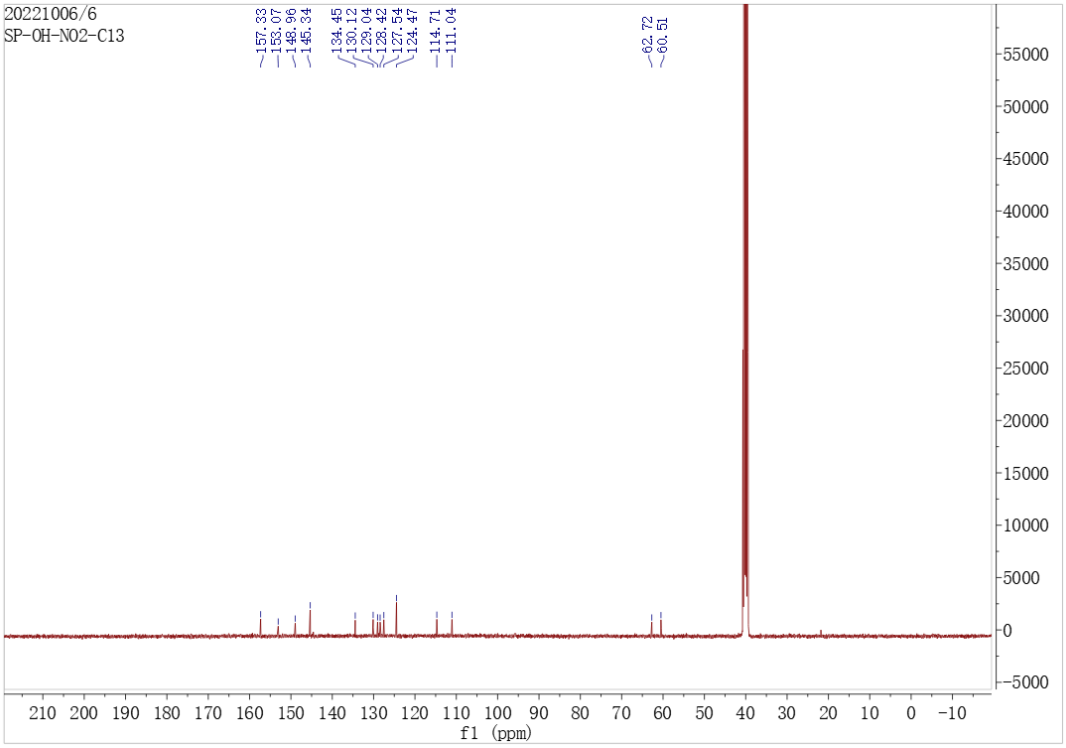


$^{13}$C NMR spectrum of SP-OH-*m*-$NO_2$

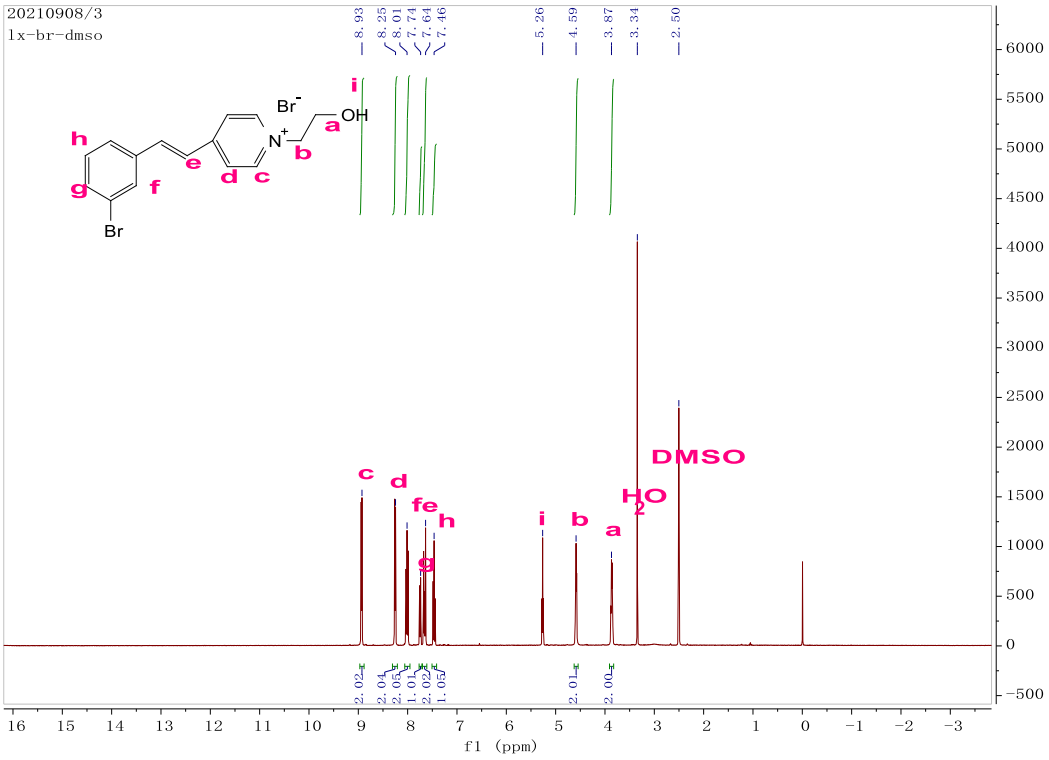


$^{1}$H NMR spectrum of SP-Br

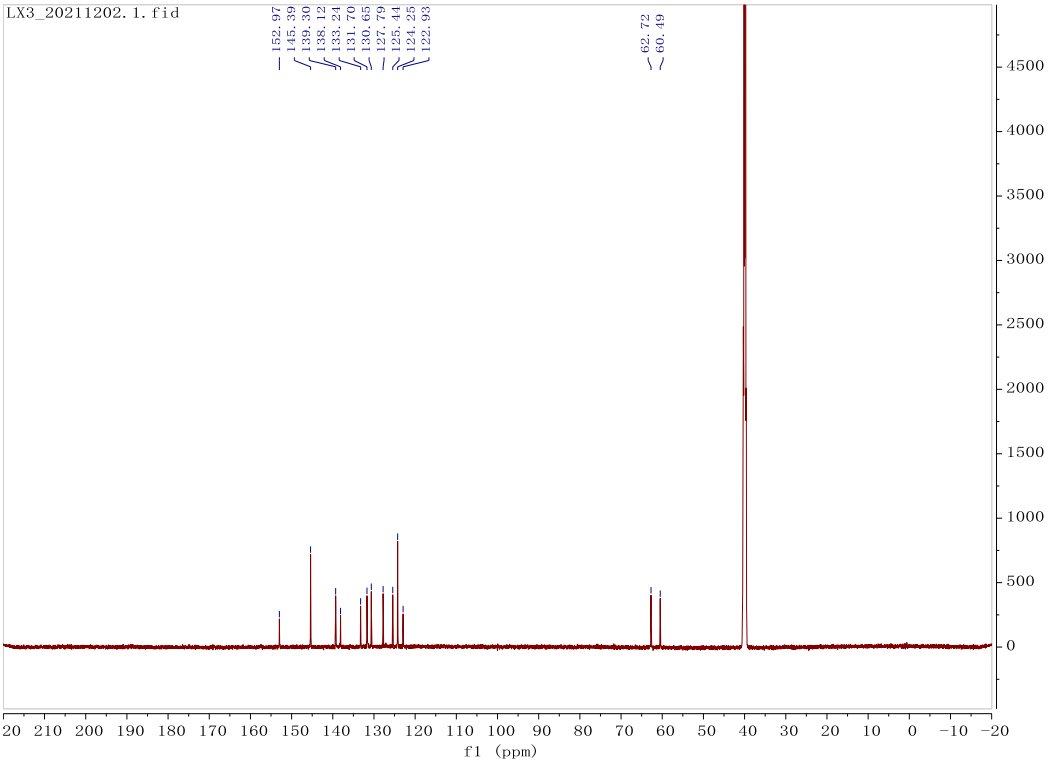


$^{13}$C NMR spectrum of SP-Br

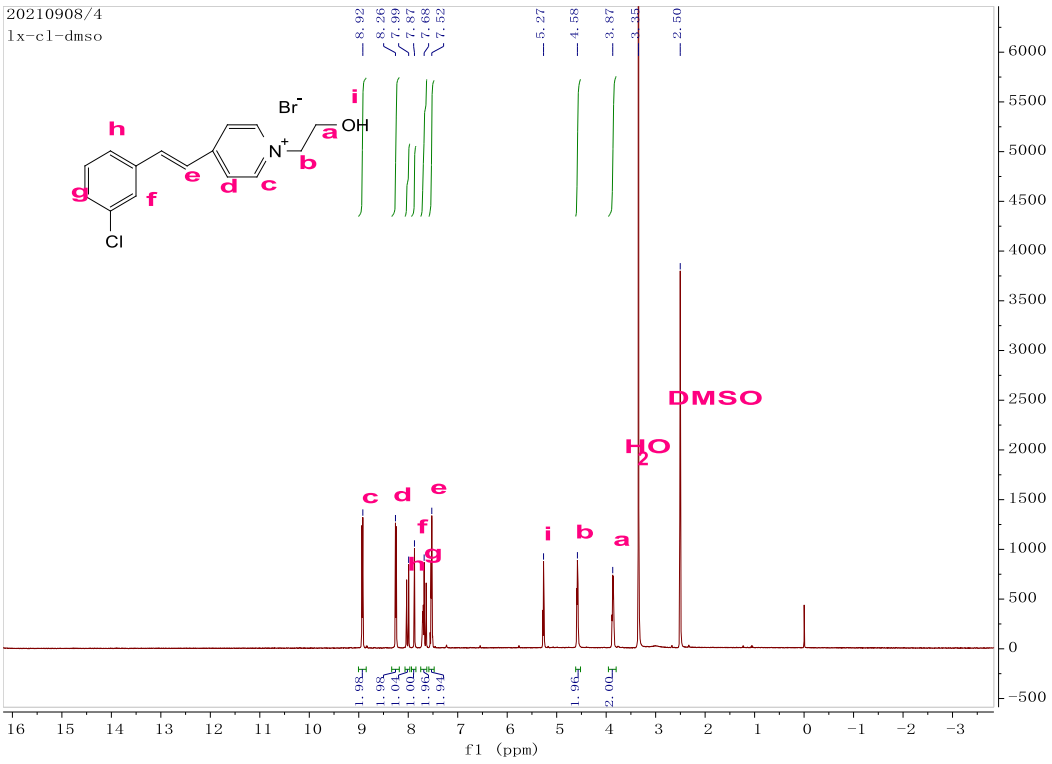


$^{1}$H NMR spectrum of SP-Cl

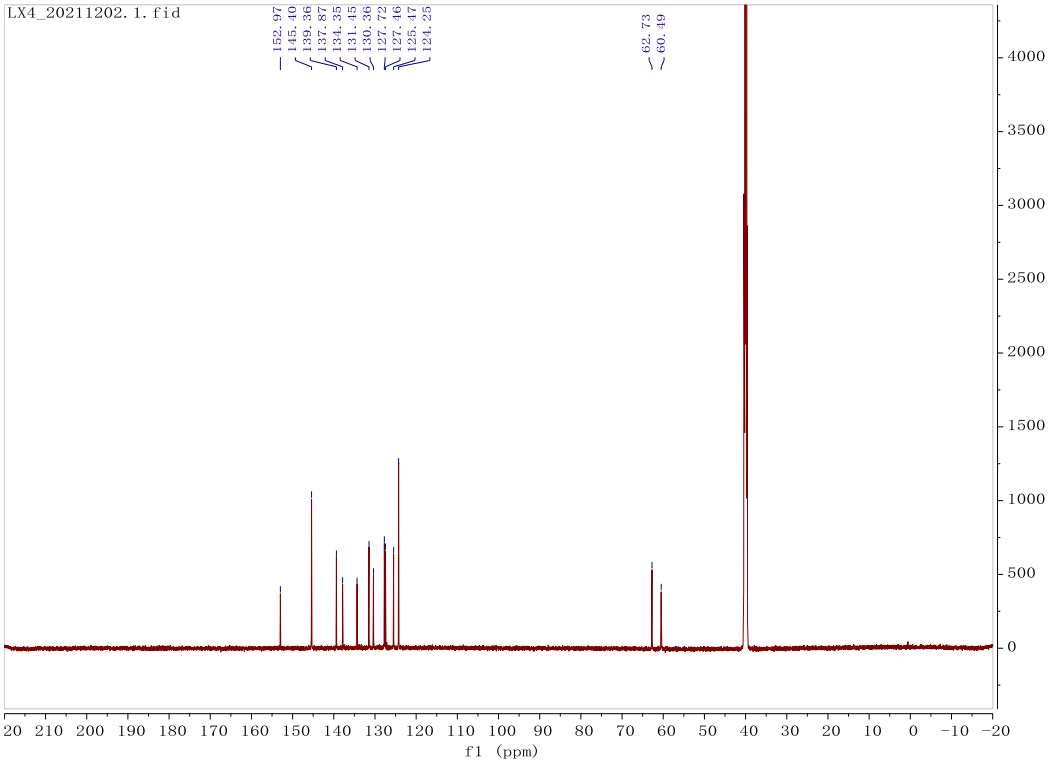


$^{13}$C NMR spectrum of SP-Cl

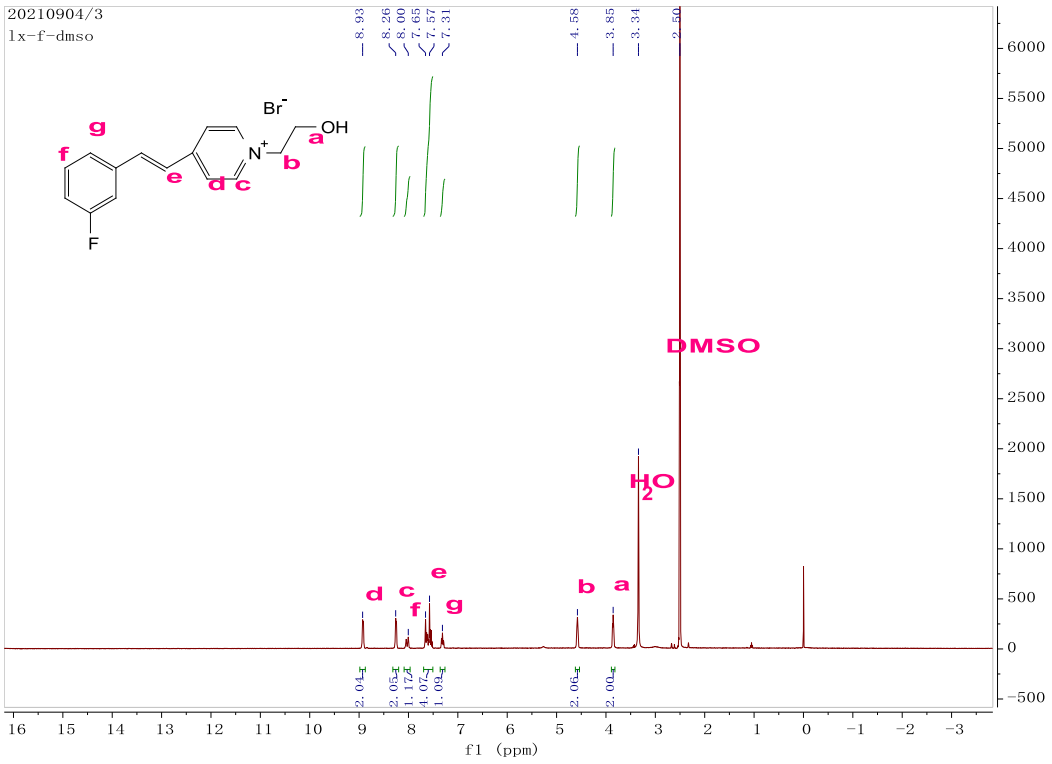


$^{1}$H NMR spectrum of SP-F

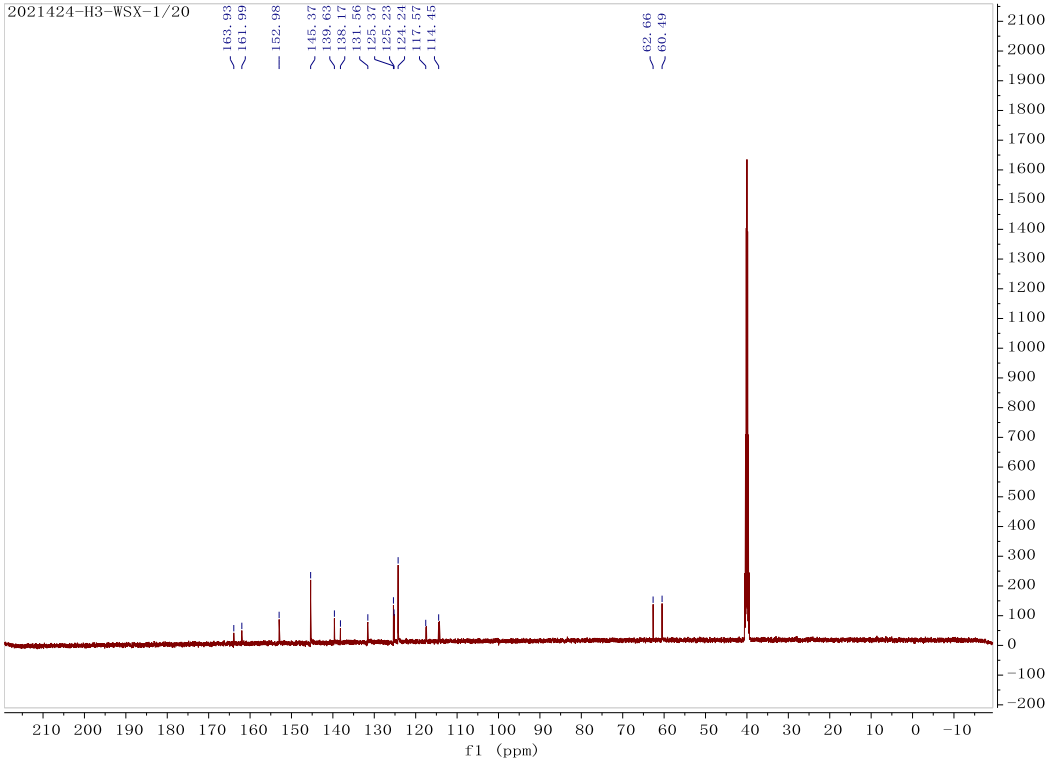


$^{13}$C NMR spectrum of SP-F

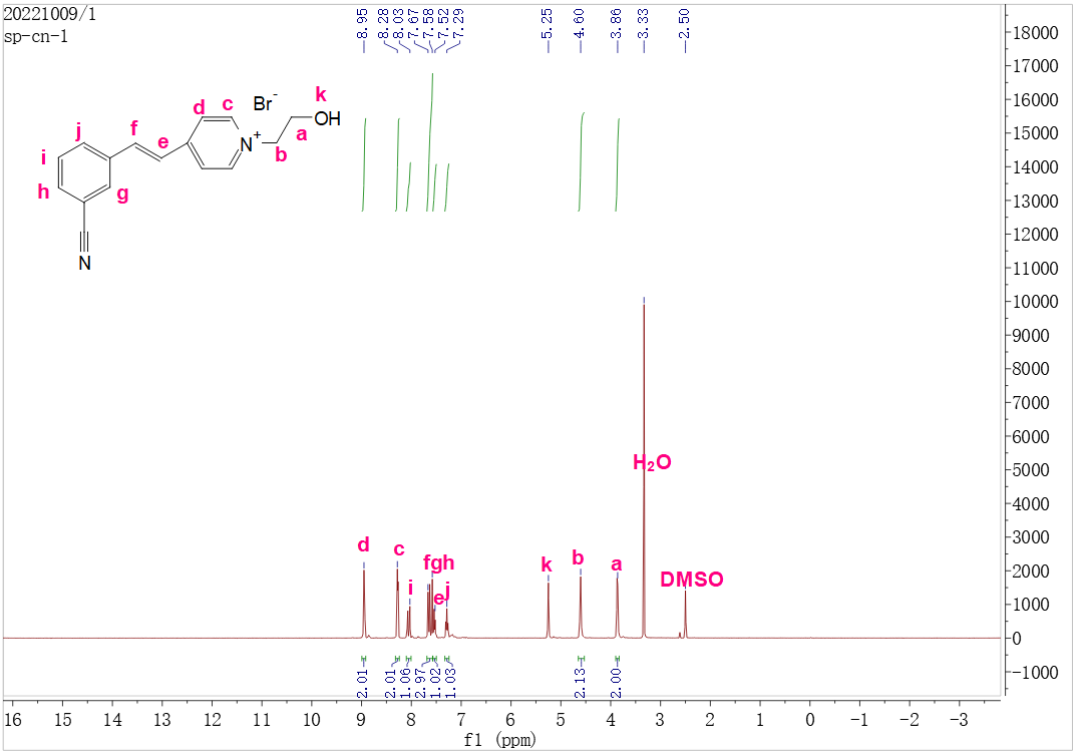


$^{1}$H NMR spectrum of SP-CN

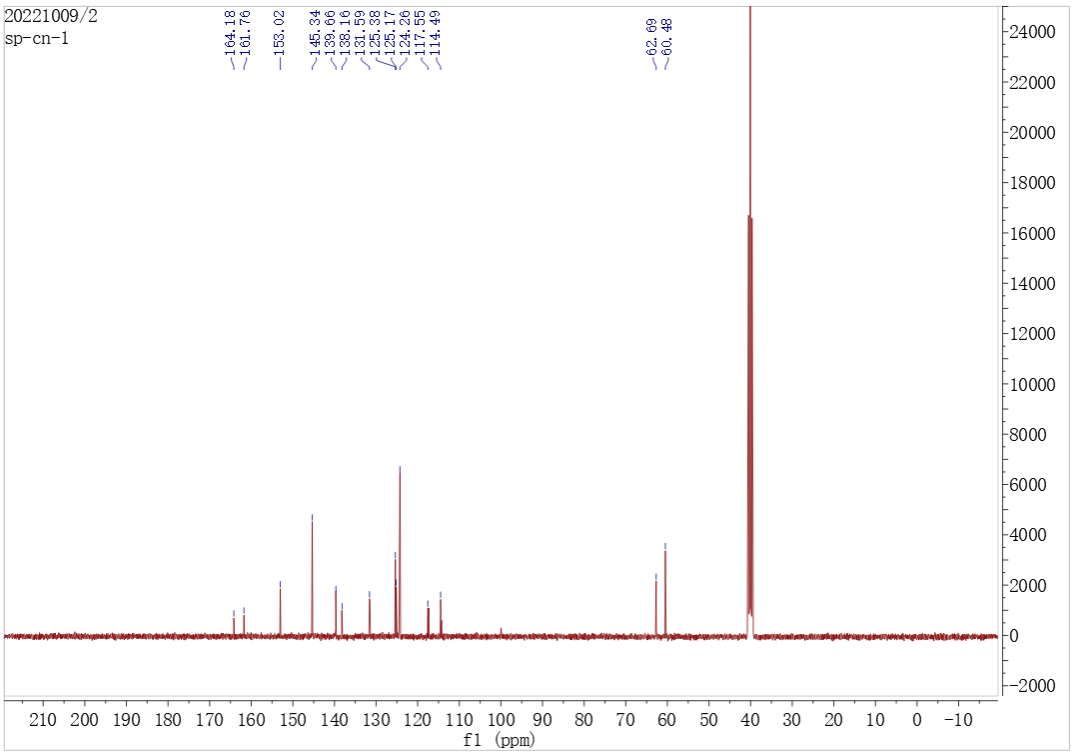


$^{13}$C NMR spectrum of SP-CN

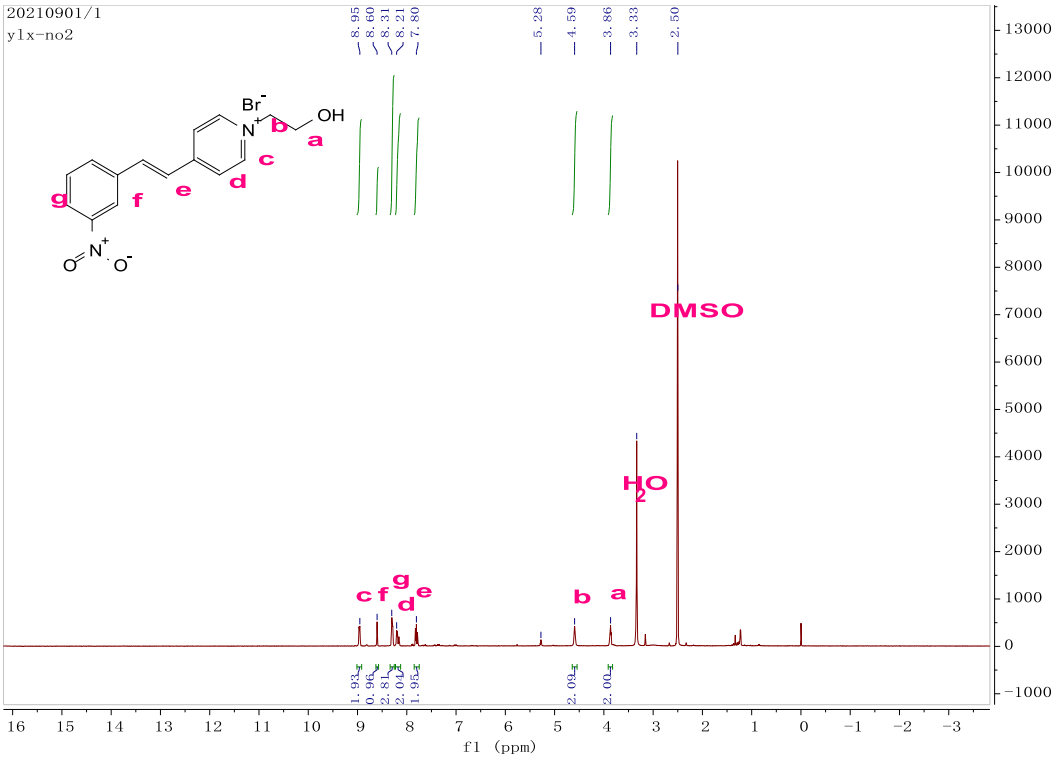


$^{1}$H NMR spectrum of SP-$NO_2$

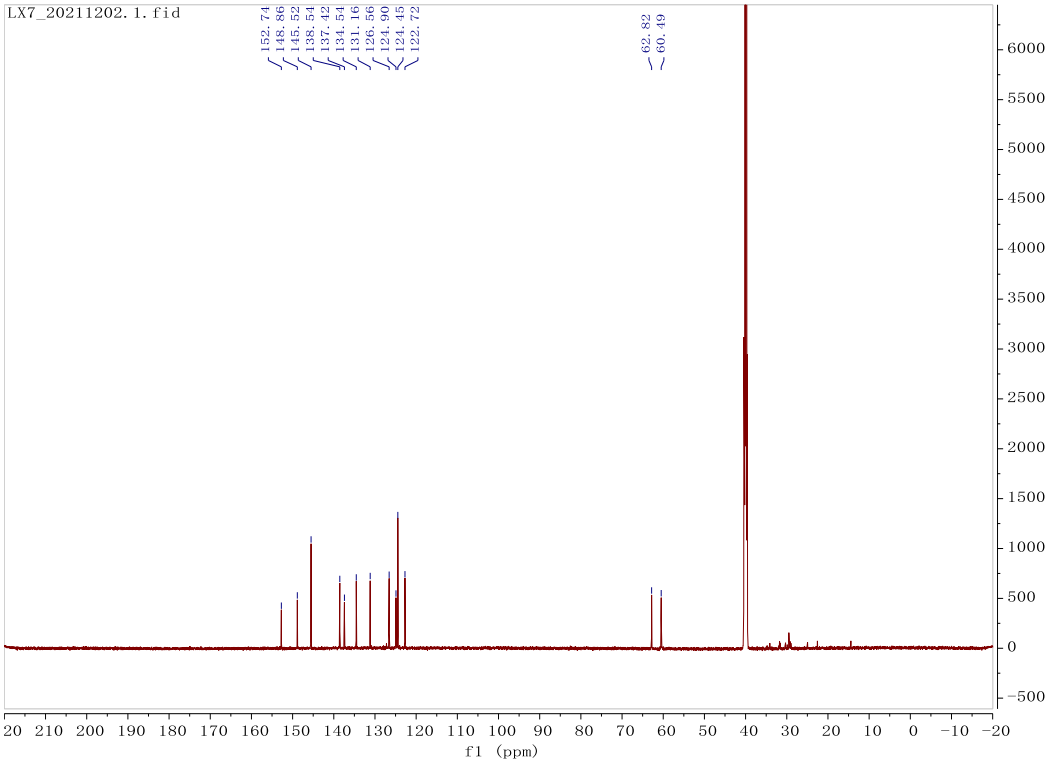


$^{13}$C NMR spectrum of SP-$NO_2$

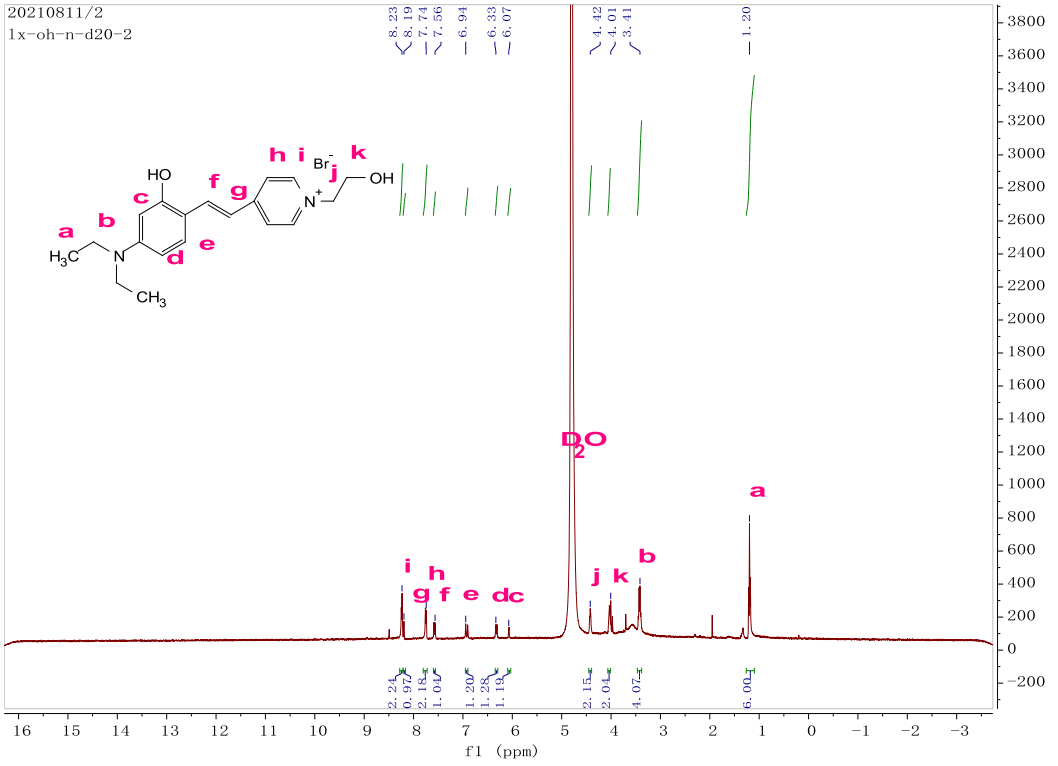


$^{1}$H NMR spectrum of SP-OH-N

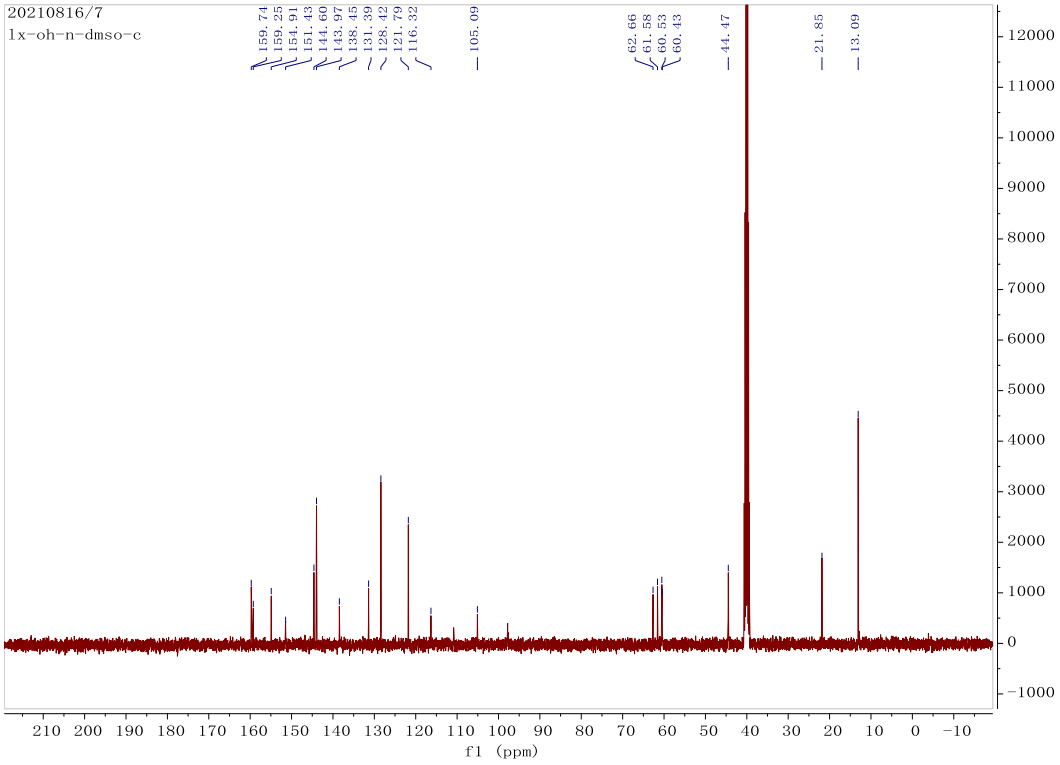


$^{13}$C NMR spectrum of SP-OH-N

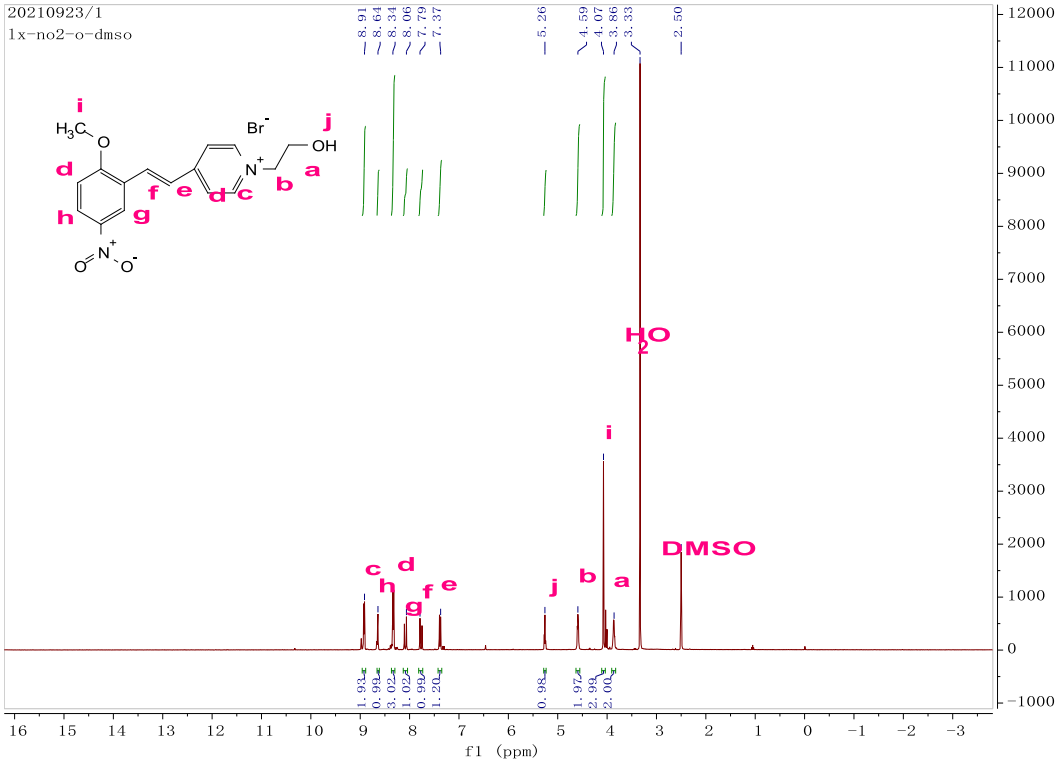


$^{1}$H NMR spectrum of SP-OMe-$NO_2$

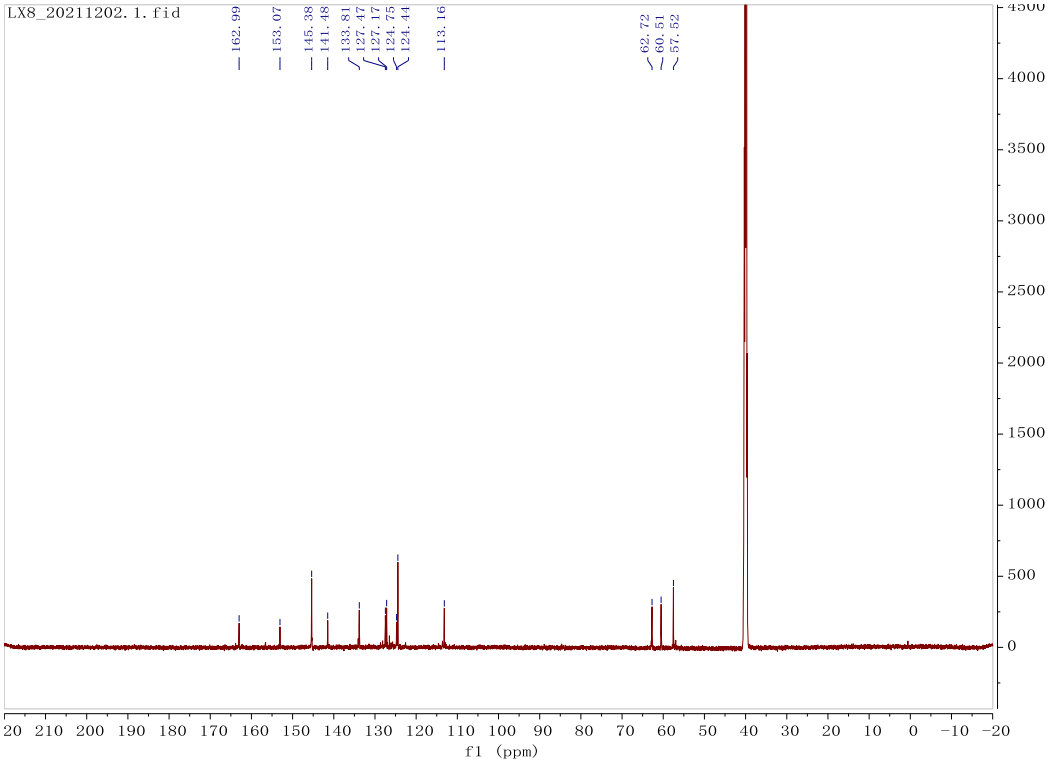


$^{13}$C NMR spectrum of SP-OMe-$NO_2$

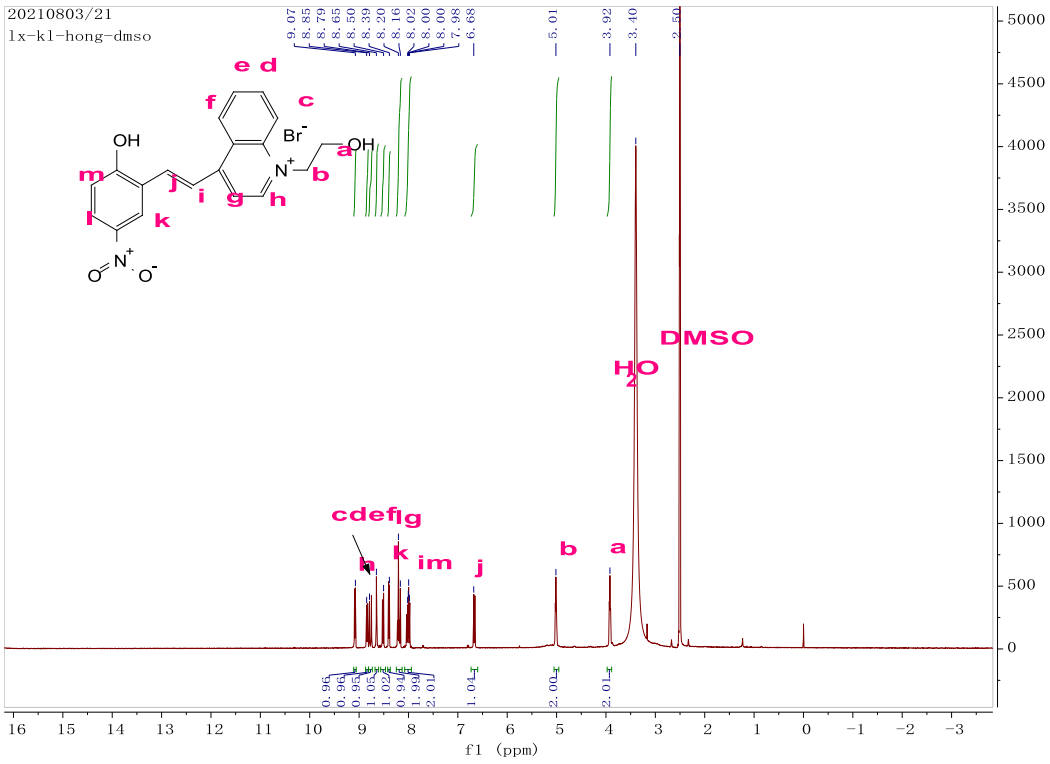


$^{1}$H NMR spectrum of SQ-OH-NO$_2$

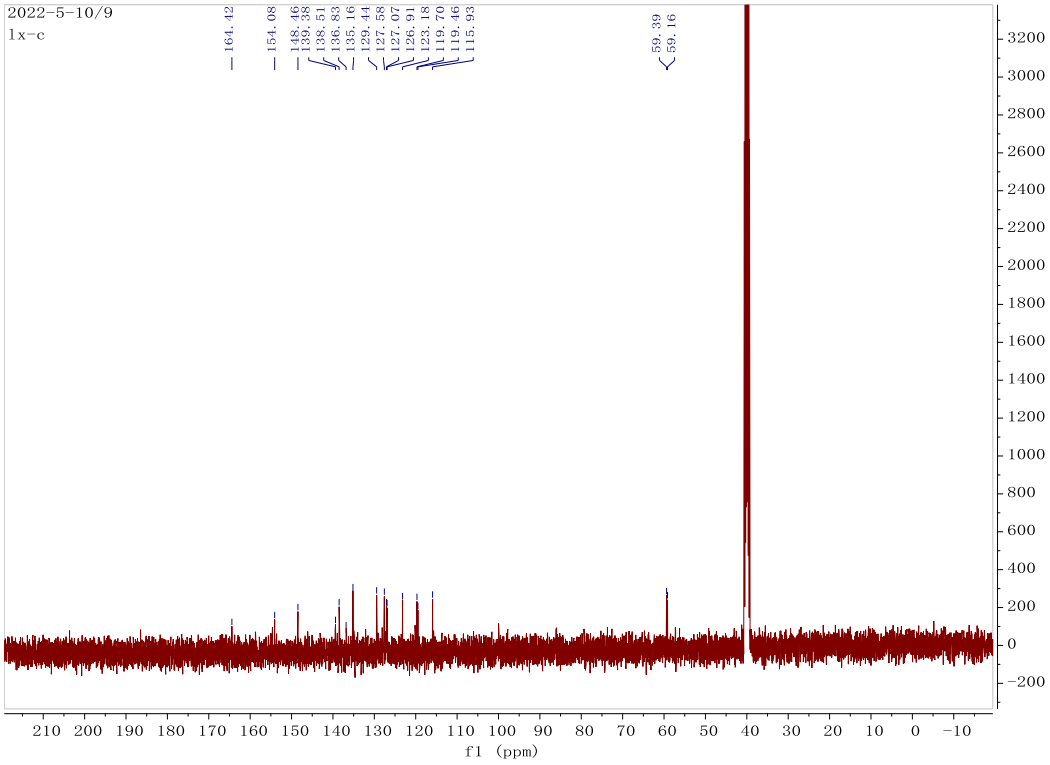


$^{13}$C NMR spectrum of SQ-OH-NO$_2$

## 6. References for Supplement Information


1 Gaussian 09, Frisch, M. J.; Trucks, G. W.; Schlegel, H. B.; Scuseria, G. E.; Robb, M. A.; Cheeseman, J. R.; Scalmani, G.; Barone, V.; Petersson, G. A.; Nakatsuji, H.; Li, X.; Caricato, M.; Marenich, A. V.; Bloino, J.; Janesko, B. G.; Gomperts, R.; Mennucci, B.; Hratchian, H. P.; Ortiz, J. V.; Izmaylov, A. F.; Sonnenberg, J. L.; Williams-Young, D.; Ding, F.; Lipparini, F.; Egidi, F.; Goings, J.; Peng, B.; Petrone, A.; Henderson, T.; Ranasinghe, D.; Zakrzewski, V. G.; Gao, J.; Rega, N.; Zheng, G.; Liang, W.; Hada, M.; Ehara, M.; Toyota, K.; Fukuda, R.; Hasegawa, J.; Ishida, M.; Nakajima, T.; Honda, Y.; Kitao, O.; Nakai, H.; Vreven, T.; Throssell, K.; Montgomery, J. A., Jr.; Peralta, J. E.; Ogliaro, F.; Bearpark, M. J.; Heyd, J. J.; Brothers, E. N.; Kudin, K. N.; Staroverov, V. N.; Keith, T. A.; Kobayashi, R.; Normand, J.; Raghavachari, K.; Rendell, A. P.; Burant, J. C.; Iyengar, S. S.; Tomasi, J.; Cossi, M.; Millam, J. M.; Klene, M.; Adamo, C.; Cammi, R.; Ochterski, J. W.; Martin, R. L.; Morokuma, K.; Farkas, O.; Foresman, J. B.; Fox, D. J. Gaussian, Inc., Wallingford CT, 2016.

2 GaussView, GaussView 6.0, Dennington, Roy; Keith, Todd A.; Millam, John M. Semichem Inc., Shawnee Mission, KS, 2016.

3 Stephens, P. J. Devlin, F. J. Chabalowski, C. F. Frisch, M. J. Ab Initio Calculation of Vibrational Absorption and Circular Dichroism Spectra Using Density Functional Force Fields. *J. Phys. Chem.* **98**, 11623-11627 (1994).

4 Zhao, Y. Truhlar, D. Density functionals with broad applicability in chemistry. *Acc. Chem. Res.* **41**, 157-167 (2008).

5 Jensen, F. Introduction to Computational Chemistry. Wiley, New York (1999).

6 Hehre, V. Radom, L. Schleyer, P. Pople, J. Ab Initio Molecular Orbital Theory. Wiley, New York (1986).

7 Woon, D. Dunning, T. Gaussian basis sets for use in correlated molecular calculations. III. The atoms aluminum through argon. *J. Chem. Phys.* **98**, 1358 (1993).

8 Foresman, J. Head-Gordon, M. Pople, J. Frisch, M. Toward a systematic molecular orbital theory for excited states. *J. Phys. Chem.* **96**, 135 (1992).

9 Wiberg, K. Hadad, C. Foresman, J. Chupka, W. Electronically excited states of ethylene. *J. Phys. Chem.* **96**, 10756 (1992).

10 Bauernschmitt, R. Ahlrichs, R. Treatment of electronic excitations within the adiabatic approximation of time dependent density functional theory. *Chem. Phys. Lett.* **256**, 454 (1996).